Elsevier Editorial System(tm) for Journal of Geodynamics
Manuscript Draft

Manuscript Number: GEOD-D-11-00031R1

Title: Tectono-metamorphic evolution of the Briançonnais zone (Modane Aussois and Southern Vanoise units, Lyon Turin transect, western Alps).

Article Type: Special Issue: Geodynamics & Orogenesis

Keywords: Western Alps, metamorphism, Ar39/Ar40 datings, subduction, collision, exhumation

Corresponding Author: Dr pierre strzerzynski,

Corresponding Author's Institution:

First Author: pierre strzerzynski

Order of Authors: pierre strzerzynski; Stéphane Guillot; Philippe-Hervé Leloup; Nicolas Arnaud; Olivier Vidal; Patrick Ledru; Gabriel Courrioux; Xavier Darmendrail

Abstract: In the central western Alps, a combined structural, petrological and 40Ar-39Ar geochronological study of the Modane-Aussois and Southern Vanoise units yields important constraints on the timing of deformation and exhumation of the Briançonnais zone. These data help to decipher the respective roles of oceanic subduction, continental subduction and collision in the burial and exhumation of the main units through time. In the Modane-Aussois unit top to the NW thrusting (D1) was followed by top to the east shearing (D2) interpreted by some as normal faulting and by others as backthrusting. Pseudosection calculations imply that D1 deformation occurred at 1.0 ± 0.1 GPa and 350 ± 30° C. Analysis of chlorite-phengite pairs yield P-T estimates between 0.15 and 0.65 GPa and between 220 and 350 °C for the D2 event. Phengites along the D1 schistosity (sample M80) yields an 40Ar-39Ar age of 37.12 ± 0.39 Ma, while D2 phengites yield ages of 35.42 ± 0.38 (sample M173) and 31.60 ± 0.33 Ma (sample M196). It was not possible to test whether these ages are altered by excess argon or not. Our interpretation is that the D1/D2 transition occurred at ~37 Ma at the beginning of decompression, and that D2 lasted until at least ~32Ma. Pseudosection calculation suggests that the Southern Vanoise unit was buried at 1.6 ± 0.2 GPa and 500-540°C. D1 deformation occurred during exhumation until 0.7 to 10.5 GPa and 370 ± 30°C. Published ages suggest that D1 deformation possibly started at ~50 Ma and lasted until ~37 Ma. D2 deformations started at P-T conditions close to that recorded in Modane-Aussois unit and lasted until 0.2 ± 0.1 GPa and 280 ± 30°C at ~ 28 Ma. The gap of 0.6 ± 0.3 GPa and 150 ± 130°C between peak metamorphic conditions in the two units was concealed by thrusting of the South Vanoise unit on top of the Modane-Aussois unit during D1 Deformation. Top to the east deformation (D2) affects both units and is interpreted as backthrusting.

Based on these data, we propose a geodynamic reconstruction where the oceanic subduction of the Piedmont unit until ~50 Ma, is followed by its exhumation at the time of continental subduction of the continental Southern Vanoise unit until ~45 Ma. The Southern Vanoise is in turn underthrusted by the Modane-Aussois unit until ~37 Ma (D1). Between 37 and 31 Ma the Modane-Aussois and Southern Vanoise units exhume together during backthrusting to the east (D2). This corresponds to the collision stage and to the activation of the Penninic thrust. In the ~50 Ma to ~31 Ma time period the main thrusts propagated westward as the tectonic context switched from oceanic to continental subduction and finally to collision. During each stage, external units are buried while internal ones are exhumed.

Cover Letter

Pierre Strzerzynski
Enseignant-Chercheur
Laboratoire de Géologie
Université du Maine,
1 Av. O. Messiaen
72080 LE MANS Cedex 09
Tel : 33(0)243833234
Pierre.strzerzynski@univ-lemans.fr

Le Mans,
23/11/2011

Dear Editor,

We propose for submission a revision of the following paper entitled Tectono-metamorphic evolution of the Briançonnais zone (Modane Aussois and Southern Vanoise units, Lyon Turin transect, western Alps) for publication within a “Geodynamics & Orogenesis” special issue of Journal of Geodynamics.

As addressed by guest editor, we introduce some more general process-oriented context for the results especially regarding the record of the transition between continental subduction and continental collision in the inner part of mountain belts. Because the paper deals not only on dating method, we do not focus especially on the problem of dating deformation.

All the authors agree with the scientific contents of the revision of this manuscript and the data is nor published or submitted elsewhere.

Syncerely,

Pierre Strzerzynski

***Detailed Response to Reviewers**

Ms. Ref. No.: GEOD-D-11-00031
Title: Tectono-metamorphic evolution of the Briançonnais zone (Modane Aussois and Southern Vanoise units, Lyon Turin transect, western Alps).
Journal of Geodynamics

Dear Chief Editor, Guest Editor and Reviewers,

Please find enclosed a new submission of the submitted paper GEOD-D-11-00031 entitled Tectono-metamorphic evolution of the Briançonnais zone (Modane Aussois and Southern Vanoise units, Lyon Turin transect, western Alps).
As addressed by guest editor, we introduce some more general process-oriented context for the results especially regarding the record of the transition between continental subduction and continental collision in the inner part of mountain belts. Because the paper deals not only on dating method, we do not focus especially on the problem of dating deformation.
As addressed by the two reviewers, a special attention has been done on the text and figure to increase the coherency of the paper. Figure calls are more precise in the text and information on the position and unit origin of sample have been added everywhere it was possible.
Numbering of the different parts has been corrected. We present our result in the same way through the paper. The results have been presented: first, by methods (structure, metamorphism and dating) then, by deformation phase (D1 and next D2) and then by studied area (Modane Aussois and next the Southern Vanoise Unit).

Changes addressed by Reviewer #1

In the following section, we present our changes according to cited remark of reviewer #1.

"Nevertheless, there are many problems related to the form of the manuscript"
Several changes on the text and the figures have been made in order to find a solution to problems related to the form of the manuscript.

"T**he tectonic model proposed for the burial-exhumation history is based on the interpretation of the pressure differences at the different stages of tectonic evolution. However, the discussion of the pressure at the different stages is not entirely clear and coherent from the text and the different diagrams. "**
To make this part of our result more readable, we rewrite the discussion were the tectonic model for the burial-exhumation history is proposed and add a new figure that forms a sketch.

"The relationship between Si content in phengite, microstructures and Ar-Ar ages are not straightforward"
We agree that there is no straightforward relationship between Si content in phengite, microstructures and Ar-Ar ages. Dating white micas from basement rock provides straightforward relationship between microstructures and mineral chemistry, however, Ar-Ar have on these samples are affected by a paragonite contribution that strongly increase the dating. To avoid this problem, we selected sample from the briançonnais cover, there is no relationship here between Si content in phengite and microstructures, but at the outcrop scale, the attribution of the structures and microstructure to the D1 or the beginning or the end of the D2 deformation phase is clear. In addition, this relative chronology is confirmed by absolute dating.

"I do not understand how the D2 deformation (west-trending top-to-the-east backthrusting) can reduce the initial pressure gap between the SVU and the MAU."
The D2 deformation can reduce the initial pressure gap between the SVU and the MAU only if high pressure metamorphism is not contemporaneous in the Southern Vanoise and Modane Aussois Unit and if a part of this gap was formed by overthrusting a previously metamorphosed unit under greater pressure (SVU) onto another metamorphic unit (MAU. Our results combined with time constrains on SVU (Gerber 2008) suggest that is the case.

"I suggest that figure 15 must be re-drawn as a sequence of cross sections explaining the burial-exhumation model discussed in the text."

We added a Figure 16 that present a possible evolution of the alpine belt and have rewrited the discussion to better discuss the burial exhumation model.

"**clear distinction between the original data and those taken from the literature**
We try to make a clear distinction between original results and data taken from the bibliography, by presenting our original data on the following parts: "structures of the Modane Aussois and Southern Vanoise Units", "Microstructure and Mineral chemistry", "Pressure and temperature conditions of the deformation events" and "Geochronological constraints on the Modane Aussois Unit". We change the title of the later part by adding "on the Modane Aussois Unit". Data taken from the bibliography are only presented and/or discussed in the following parts: introduction, geological setting and discussion.

Changes addressed by Reviewer #2

According to report of reviewer #2, we present our changes following the structure of the paper.

Introduction
We developed the geodynamic questions and the way we will try to answer the question in the introduction. We provide a description of the Alpine belt structures as light and understandable. This should lead the paper to be understandable by wider range of geologists. In addition, we change the reference to the foreland and hinterland by absolute direction in order to avoid reference relative only to collision stage.

1 Geological Setting
Corrections have been made as addressed by reviewer 2.

2 Methods
In the present paper, we only limited the use of pseudosection to the metamorphic peak condition assuming that the rocks are fully or nearly fully reequilibrated at these conditions. Concerning chlorite phengite methods, Fe is taken into account as in previous studied (see Vidal et al., 2005). This was a mistake of the first version of the paper.

3 Structures of the Modane Aussois and Southern Vanoise unit
Tectonic scenario is limited within the text and figure to D1, nappes stacking and duplex formation, D2 top to the E and SE deformations and then late tiltings. In addition, we add more precision on the call of figures as asked. That's especially the case for the figure 4 (field picture), figure 5 (cross section A or B) and figure 8 (stereoplots) where each part of the figures is labelled and called in the text.
In a same way, we add two stereo plots to the figure 8 to present the orientation of the D1 and D2 structure and two pictures on the figure 4 to describe the D1 and D2 structure of the Southern Vanoise Unit.
We add a table and several explanations on unfolding D1 lineation along two different axes: N30° horizontal for the D2 deformation and N90°-horizontal for late tilting.
We correct the position of the cross-section on the Figure 6.

4 Microstructures and mineral chemistry
We rewrite the mineral description and provide as much link as possible to figure and table.
We present Si vs Na diagram for phengite as the paragonite component of white micas play an important role from dating. The diagram highlights Si change from a deformation phase to another and the possible problems from dating.
Glaucophane evidence are provided both with microphotographs (Figure 9A, B, C) and with chemical analyses.

5 P and T condition of the deformation event
Explanations on the pseudosection construction are presented in the 2. Method section, we do not redraw the section. In the present paper, we only limited the use of pseudosection to the metamorphic peak condition assuming that the rocks are fully or nearly fully reequilibrated at these conditions.
We present a corrected version of the pseudosection on the Southern Vanoise Unit assuming no Jadeite and Si > 3.4 for the metamorphic conditions of D1. This does not change the Pressure estimates and provides better constrain on temperature. In the present paper, we discuss the occurrence of the metamorphic gap both on quantitative and qualitative observations.

In the previously submitted paper we have presented chlorite phengite result of different rock sample from the Modane Aussois Unit on the same pseudosection. We understand that it is incorrect. We added a third pseudosection build for non glaucophane bearing micaschist of the Modane Aussois unit (sample F21-5) and present on this sample only chlorite phengite result from sample F25-5.
Concerning chlorite phengite methods, Fe is taken into account as in previous studied (see Vidal et al., 2005). This was a mistake of the first version of the paper.

6 Geochronological constraints
A precise localisation of the sample is available on the figure 5. In addition we add in the text a more precise description of the sample we explained why we selected only samples from the briançonnais cover. Within the Modane Aussois Unit and especially within quartzite slice, it is easier to recognize D1 and D2 structures at the outcrop or the map scale than at the thin section scale. This leads us to date structurally simple samples without large amount prealpine phengite. Unfortunately, the approach does not provide relative chronological arguments at the thin section scale.

We add, a table with all the result of Ar-Ar dating together with Ar^{38}/Ar^{39} , Ar^{37}/Ar^{39} vs Ar released spectra to the figure 12 This lead us to have a better discussion on datings according to the relationship between composition and age. One age is constrained with less that 70% of Ar released has been especially discussed in the text.

7 Discussion
We rewrite and change the structure of the discussion. Once again a special attention has been done on the coherency between the text and the figure. We also provide more precise figure call in the text.
A short introduction resumes the Metamorphic result and highlight (1) a similar continental subduction context of burial for the Southern Vanoise and The Modane-Aussois units and (2) a decrease of the subduction dynamic as the Modane-Aussois not buried very deep.
Discussion contains now the following parts:

<u>P-T-t-d path of Modane-Aussois unit</u>.
It is based on our own structural, metamorphic and geochronological results.

<u>P-T-t-d path of Southern Vanoise unit</u>
It based on our PTd dataset and time constrain taken from the literature. By doing this, we hope that a clear distinction will be seen between our own results and those taken from published studies.

<u>Metamorphic gap and the origin of the contact between Modane-Aussois unit and Southern Vanoise unit.</u>
Changes on the metamorphic estimate confirm the occurrence of this gap. Pt diagram presented on the figure 15 indicate that the timing of the gap formation mostly during D1 deformations. This leads us to propose that prior to the D2 deformation; the Southern Vanoise has been thrusted onto the Modane-Aussois Units.

<u>a tectonic and metamorphic evolution of the Piedmont, Southern Vanoise and Modane-Aussois units</u>
Considering the absolute timing of the deformation phase together with PTtd results of Agard et al. (2002) on the Piemont Unit, we propose a possible evolution along an E-W cross section of the western Alps between 50 and 30 Ma. This is presented on a new figure (Figure 16) where successive very interpretative cross sections are presented. The tectonic evolution of the studied area is replaced in the context of the Alpine evolution: continental subduction during D1 followed by continental collision during D2

<u>The signification of the top to the E tectonic phases</u>
We have revised our arguments on the signification of D2 deformations. Geometric arguments are the D2 foliation dip as a whole, to the west witch is compatible with backthrust. The timing of the D2 deformation is the second argument: D2 deformations are coeval with collision processes. Considering this, we propose: “(1) the collision wedge becomes thicker not only by the underthrusting of the external unit and there is a contribution of the internal part of the belt into the thickening of the belt. (2) Backthrusts that contribute to the thickening of the belt together with motions along the Penninic thrust are not only limited to the eastern boundary of the belt between the alpine belt and the Pô plain.”

Conclusions

We rewrite the conclusion on the basis of the new discussion.

Figure

Figure 2: few modification have been done on this figure, It illustrate the relationship between the main tectonic unit and we think that lithological information must be restricted to the geological map (Figure 5).

Figure 4 : Correction have been made on the deformation phase label and on the caption. We add two new picture in order to show structure from the Southern Vanoise Unit. Label

Figure 5: In the studied area, several factors make the geological map especially difficult to read:
(1) Structure and topography have a complex interplay as they have in many places a similar orientation, that especially the case for the quartzite slice on the Modane Aussois unit and also for the D2 structure in the Southern Vanoise Unit.
(2) The building of the Geological map (Figure 5) and crosssection (figure 6) have been done in the special context of the Lyon Turin Projet: field work has been made at high resolution and more than 10km cumulated long of borehole have been used.
The present map and crosssection try to give a geometrical coherency both in surface and in depth of these very observations.
In addition, D1 and D2 foliations are variously expressed depending on the rock formation. This contributes to a very heterogeneous spatial repartition of measurements making foliation map not easy to read.
To make a more readable map, topographic information associated with foliation maps should be presented on a 1/10000 scale support in association with borehole logs and borehole stereodiagram. Numerous cross sections should be presented in the context of an independent article. Because the submitted paper does not only focus on structural aspect, we decided to present our final map and cross section on the studied area and to discard a large amount of dataset used for buiding the maps and the cross section.

Figure 6 : we corrected the position of the cross section on the geological map, in addition we added more localities information and more structure name in order to provive more links between the text and the figures.

Figure 8: it has been completed by two stereodiagram leading to present D1 and D2 structures of the Southern Vanoise Unit and stereodiagram A and B have been completed by a table that present rotation angle and rotation angle axis for unfolding D1 lineations.

Figure 9: we added uncrossed light picture for each sample ample, deleted the interpretations and added a new photography of sample M266 that is suitable for the text.
Figure 10 11: asked modifications have been made.

Figure 12 : we added caption for the figure 12 B, C and D and provide a more suitable label to better call the figure in the text.

Figure 13: we added a pseudo section for sample F21-5 and simplified symbols. The diagram are the result of pseudo section model, we only change the label size in order to make it more readable.

Figure 15 : Corrections have been applied on unit and structures labelling. No tectonic sketches have been added however a new figure (16) depict a possible evolution of these units.

Figure 16: It is a new figure depicting a possible evolution of the internal alps between 50 and 30 Ma.

*Manuscript
Click here to view linked References

Tectono-metamorphic evolution of the Briançonnais zone (Modane-Aussois and Southern Vanoise units, Lyon Turin transect, western Alps).

Pierre Strzerzynski[ab*], Stéphane Guillot[c], Philippe-Hervé Leloup[d], Nicolas Arnaud[e], Olivier Vidal[b], Patrick Ledru[f], Gabriel Courrioux[g], Xavier Darmendrail[h]

[a] LPGN, CNRS UMR 6112, Université de Nantes, rue de la Houssinière, 44322 Nantes Cedex 3, France
[b] Laboratoire de Géologie UFR Sciences et Technique, Université du Mans, Avenue O. Messiaen 72000 Le Mans, France
[c] ISTerre , Université Grenoble I, CNRS, 1381 rue de la Piscine. 38041 Grenoble, France
[dc] LST, Université of Lyon, CNRS, 2 rue Dubois, 69622 Villeurbanne, France
[e] Géosciences Montpellier, CNRS, Place Eugène Bataillon 34095 Montpellier Cedex 5, France
[f] AREVA Business Unit Mines, Département Géosciences, 1 place Jean Millier, BAL 0515A, 92084 Paris La Défense, France
[g] BRGM/DR-D BP 6009 45060 Orléans cedex 02 France
[h] LTF Lyon Turin Ferroviaire, 1091 Avenue de la Boisse, - BP 80631 -73006 Chambéry, France.

* corresponding author: Pierre STRZERZYNSKI
e-mail adress: <Pierre.Strzerzynski@univ-lemans.fr>, fax number: +33 4 72 44 85 93

Introduction

Although the formation of high pressure (HP) and ultrahigh pressure (UHP) rocks is an integral process occurring in oceanic or continental subduction (Ernst, 2001), their exhumation is a transient processes occurring during oceanic subduction or during continental collision (Ernst, 2001; Agard et al., 2008). The transition from oceanic subduction to continental collision is marked by the subduction of the continental margin, still attached to the downgoing oceanic slab during when, HP To UHP rocks of continental rocks are produced (Chopin, 1987) and worldwide exhumed (Guillot et al., 2009). Moreover, this period is crucial in the evolution of mountain belt as it records a decrease of the plate convergent rate, the progressive transition from marine to continental sedimentation due to continental uplift of the lower plate and the transition from low temperature to middle temperature geothermal gradient (Guillot et al., 2003). Understanding the exhumation of high and ultra-high pressure (HP to UHP) rocks is a major challenge in our knowledge of plate convergence and mountain building processes. Exhumation of HP to UHP rocks results from the interaction of boundary forces, buoyancy, rheology, geometry of the subduction channel and surface processes (Jolivet et al., 2003; de Sigoyer et al., 2004; Agard et al., 2008; Guillot et al., 2009). The timing of exhumation with respect to the onset of continental subduction has important bearings on the exhumation processes (Brun and Faccenna, 2008: Guillot et al., 2009). Models proposed for the exhumation depend upon the orogenic context i.e. subduction or collision. Pro- and back-thrustings coupled with strong erosion and the formation of

foreland basins take place during collision. A wide variety of exhumation model have been proposed during the subduction stage : channel flow (Cloos, 1982), corner flow (Platt, 1986), extensional collapse (Dewey et al., 1993), thrusting towards the foreland (Steck et al., 1998), buoyancy assisted by erosion and tectonics (Chemenda et al., 1995), compression of a soft zone between two rigid blocks (Thompson et al., 1997), serpentinite channel (Guillot et al., 2001), and coaxial extension associated with a decoupling fault (Jolivet et al., 2003).

The Western Alps are a good example for studying the exhumation processes of HP to UHP metamorphic rocks as early HP-LT metamorphic relics have been widely preserved. It is a curved orogenic belt consisting of a nappe stack of continental terranes, that are from the top to the bottom Austroalpine, Internal Crystalline Massifs, Briançonnais zone and External Alps (Figure 1). Two oceanic domains separate these continental domains (Figure 1): the Piedmont zone between the Austroalpine and the Internal Crystalline Massifs and the Valais oceanic unit squeezed between the Briançonnais zone and the external Alps along the Penninic Thrust (e.g. Schmid and Kissling 2000, Rosenbaum et al., 2005).

In the internal part of the belt, HP to UHP metamorphic rocks formed and exhumed during distinct periods: 65 Ma for the Austroalpine massif (Duchêne et al., 1997), between 65 and 45 Ma for the Piedmont zone (Agard et al., 2002, Lapen et al., 2003), between 45 Ma and 35 Ma for the Internal Crystaline Massifs (Duchêne et al., 1997, Meffan-Main et al., 2004) and the Briançonnais zone (Markley et al., 1998, Freeman et al., 1997) and at 35 Ma for the Valais unit (Bousquet et al., 2002). The variation in metamorphic ages and a geothermal gradient lower than 10 $°C.km^{-1}$ in these rocks suggest that such nappes formed in a subduction wedge from 65 to 35 Ma (Rosenbaum et al., 2005; Ford et al., 2006; Lardeaux et al., 2006; Gabalda et al., 2008). The transition from subduction to collision is dated at ca. 35Ma and is associated with the activation of the Pennine thrust (Schmidt and Kissling, 2000, Pfiffner et al., 2002, Leloup et al., 2005, Rosenbaum et al., 2005, Beltrando et al., 2010; Dumont et al., 2011). Recently this age has been confirmed on the basis of P-T-t estimates of alpine metamorphism in the External zone (Rolland et al. 2008, Simon-Labric et al., 2009). Such event is associated with the formation of backthrusts from the internal part of the belt (Tricart, 1984; Platt et al., 1989; Schmidt and Kissling, 2000; Tricart and Sue, 2006) to the boundary between the Pô plain and the alpine belt (Carrapa and Garcia-Castellanos, 2005, Escher and Beaumont, 1997, Roure et al., 1990).

In the internal part of western Alps, tectonics associated with exhumation is polyphased. Early, top to N or NW direction of nappe emplacement and shearing accommodated the earliest and rapid exhumation of the HP and UHP continental units. This tectonic phase (D1) is observed and interpreted everywhere as a thrusting phase (Agard et al., 2002, Markley et al., 1998, Bousquet et al., 2002, Reddy et al., 2003, Bucher et al., 2003, Ganne et al., 2007; Wheller et al, 2001, Le Bayon and Ballèvre, 2006).

The D1 nappe stack is often affected by top to the east or SE shearings (D2). In the Piedmont zone, these D2 structures accommodate a significant part of the exhumation in a context of extension (Agard et al., 2002, Reddy et al., 1999, Rolland al., 2000; Ganne et al., 2006; 2007). A late Eocene age (> 35 Ma) is proposed for these structures (Agard et al., 2002, Reddy et al., 1999).

Others top to the east or southeast structures occurred after the major exhumation phase. Some of these structures are responsible for the fan shape of the western Alps and are interpreted as back-thrusts (Tricart, 1984, Platt et al., 1989, Escher and Beaumont, 1997, Le Bayon and Ballèvre, 2006, Tricart and Sue, 2006). An Oligocene Age (~ 33-25 Ma) is attributed to these structures by analogy with other ones observed further SE at the rear of the Pô plain (Carrapa and Garcia-Castellanos, 2005, Roure et al., 1990) and that are coeval with the formation of foreland basins (Schmidt and Kissling, 2000, Pfiffner et al., 2002, Ford et al., 2006). Backfoldings related to backthrusting or to normal faulting are also described in the

Briançonnais units (Bucher et al., 2003; Tricart and Sue, 2006; Ganne et al., 2006). Following the successive phases of ductile deformation, two phases of brittle deformation took place, producing orogen parallel extension followed by orogen perpendicular extension (Strzerzynski et al., 2004, Malusa et al., 2005; Champagnac et al., 2006; Sue et al., 2007).

In the present study, we focus on the intermediate zone of the continental orogenic system between the internal zone and the external zone. In this area both subduction and collision related structures are found (Tricart, 1984; Tricart and Sue, 2006; Gabalda et al., 2008; Ganne et al., 2007), giving the opportunity to decipher their respective role in the exhumation of HP units. We conducted a combined structural, petrological and geochronological study in order to relate the deformation phases with the P-T-t evolution and to discuss how and when the continental crust is exhumed in the western Alps. We review the stratigraphy, structure and metamorphic evolution of the area, and present new P-T estimates and ^{40}Ar-^{39}Ar ages. We finally propose a tectonics and metamorphic evolution of the internal western Alps between 45 and 30 Ma.

1. Geological setting

- *Location of the studied area*

The Studied area encompasses Modane and Aussois cities in the Maurienne Valley (Figure 1). It consists of Briançonnais basement and cover over-thrusted to the south and the east by the Piedmont and Gypse nappes (Figure 2). The Piedmont nappe emplacement took place during the early top to the NW tectonic event (Ganne et al., 2007). To the West, a tectonic contact separates the Briançonnais and the Houiller zones (Figure 1). This contact is interpreted either as a major detachment zone (Caby, 1996) or a refolded thrust (Aillères, 1996). Within the studied area we distinguish three different units (Figure 2): the Modane-Aussois unit mostly composed of Permian and Triassic sediments, the Southern Vanoise unit composed of Briançonnais basement, and the Dent Parrachée unit composed of Mesozoic sediments. An early top to the NW tectonic contact is generally accepted for the emplacement of the Dent Parrachée unit onto the Southern Vanoise unit (Ellenberger, 1958, Platt and Lister 1985, Ganne et al., 2005). It is not clear whether the Dent Parrachée unit is locally in direct contact with the Modane-Aussois unit, or only tops the Southern Vanoise unit (Figure 2). The contact between the Modane-Aussois and Southern Vanoise units, coresponding to a top to the east shear zone has recently been interpreted as a detachment (Ganne et al., 2006; 2007, Gerber 2008).

- *Rock formations*

Rocks formations of the Briançonnais zone have a continental origin and consist of basement rocks covered by a sedimentary cover.

Basement rocks consist of a complex mixture of micaschists, gneisses and volcanic rocks interpreted as an old volcanoclastic sequence (Figure 3, Gay, 1971). Rocks classification established within the Ambin Massif (Figure 1) have been successfully applied in the studied area (Debelmas et al., 1989). The deepest levels are called the Clarea group (Gay, 1971); they exhibit relics of an ante-alpine amphibolite-facies metamorphic event (Bertrand and Leterrier 1997, Bertrand et al., 2000). In contrast, there is no evidence of pre-alpine metamorphism in the upper part of the basement called the Ambin unit (Gay, 1971, Bocquet et al., 1974, Borghi et al., 1999).

Three series have been distinguished within the sedimentary cover relative to the opening of the alpine-tethys ocean: pre-rift series from Permian to Triassic and post-rift series

from Dogger to Eocene separated by either Liassic syn-rift deposits or by a major unconformity (Figure 3). The basal part of the pre-rift series consists of siliceous metasediments, from base to top outcrop: conglomerates, micaschists, phyllites quartzites and white quartzites (Figure 3, Debelmas et al., 1989). The conglomerate contains pebbles of quartz, carbonates and schist in a quartzitic matrix. Micaschists and micro-conglomerates with characteristic red quartz pebbles form the so-called "Etache group" or "Permo-Trias" (Ellenberger, 1958). They grade into a 100m thick white quartzites layer that show well-preserved sedimentary structures (Figure 4a). The ages of the metasedimentary group is poorly constrained. The top of the pre-rift series consists of schists, carbonates and gypsum deposits containing middle to upper Triassic fossils (Ellenberger, 1958). The Carnian gypsum layer acts as a major décollement decoupling the middle Triassic rocks called the Esseillon group, from the upper Triassic dolomite.

The syn-rift series are only observed in the Dent Parrachée group (Figure 3). They consist of Liassic carbonates and calcschists. Elsewhere in the Modane-Aussois area, syn-rift period is underlined by a discontinuity.

The post-rift series consist of carbonates and schists deposited between the Dogger and the Eocene (Figure 3). Sedimentation is characterized by numerous unconformities in particular during the Early Cretaceous. The post-rift series lies both on top of the Liassic syn-rift Dent Parrachée series, and on top of upper Triassic dolomite of the Roc du Bourget (Ellenberger, 1958, Megard-Galli and Baud, 1977) (Figure 2).

- *Tectonics, metamorphisms and geochronology.*

Previous studies mostly focused on the Southern Vanoise basement rocks. The Southern Vanoise unit is characterized by a polyphased tectonic evolution with early top to the NW deformation followed by top to the east deformation (Platt and Lister 1985, Ganne et al., 2005, Gerber 2008). Superposed deformation phases lead to the formation of kilometer scale interference folds within the basement units (Ganne et al., 2005).

Platt and Lister (1985) followed by Ganne et al., (2007) and Gerber (2008) proposed relationships between the deformation events and the P-T evolution. For Platt and Lister (1985): 1) P-T peak is defined by the association jadeite + quartz and glaucophane + lawsonite; suggesting pressure of ~1.2 GPa and temperature ~300°C. 2) the top to the NW deformation postdates de metamorphic peak and takes place under blueshist facies conditions. 3) The top to the east deformation occurred later under greenschist facies conditions accommodating a minor amount of exhumation. For Ganne et al., (2007) and Gerber (2008): 1) P-T peak conditions are constrained by the association garnet, jadeite, phengite, paragonite, glaucophane, chloritoid and clinozoisite giving pressure and temperature conditions of 1.8 ± 0.1 GPa and 450 ± 50°C. These results have been confirmed by peak temperature estimates obtained from Raman spectroscopy of Carbonaceous Material (Gabalda et al., 2008). 2) The top to the NW deformation occurred during the P-T peak. 3) Top to the east deformation started under blueschist facies conditions as evidenced by the presence of a second generation of glaucophane and accommodates a significant amount of exhumation.

The Eocene Age of the last sedimentary formation of Vanoise, place an upper bound on the age of metamorphism and related deformations. Various geochronologic methods have been used to try to constrain the age of the deformation phases. Ar^{40}/Ar^{39} step heating on phengite of basement samples does not provide any plateau age and cannot be interpreted simply (Ganne 2003). Rb/Sr on phengite and calcite suggest an age of 34-35Ma for the D2 shear zones (Ganne et al., 2007). From Ar^{40}/Ar^{39} laser ablation ages on phengite Gerber (2008) proposed that top to the NW tectonic phase occurred between 50 and 43Ma and was immediately followed by the top to the east tectonic phase ending at 30-28Ma.

There is a consensus on the signification of the early tectonic phase: top to the NW thrusting in the Brianconnais zone occurred in a context of shortening related to continental subduction. However, different interpretations have been proposed for the top to the east tectonic phase. On one hand, it is interpreted as backthrusts in a context of frontal continental collision (Platt and Lister 1985, Platt et al., 1989). On the other hand, top to the east structures are interpreted as detachment associated with large amount of exhumation prior the frontal continental collision (Ganne et al., 2005, Gerber 2008).

2. Methods

We conducted a structural analysis based on a micro-, meso-structure analysis, geological mapping, and a metamorphic study associated with Ar^{40}/Ar^{39} dating. Samples were taken from the basement and the metasedimentary cover both at the surface and from drill holes performed in the frame of the Lyon - Turin tunnel project (Figure 5). Mineral compositions (Table 2) were determined using the CAMECA SX100 microbeam of the Brest University (15kV – 20nA). Standards were albite (Na), orthoclase (K), corundum (Al), wollastonite (Ca, Si), forsterite (Mg), MnTiO3 (Mn, Ti), Fe2O3 (Fe) and Cr2O3 (Cr). Bulk compositions of samples were determined using X-ray fluorescence at the Earth Science Laboratory of Lyon (table 3).

- P-T estimates

Metamorphic paths were estimated using pseudo-section with PERPLEX Software (Connoly, 1990) and chlorite-phengite-quartz P-T calibration (Vidal et al., 2001). Pseudo-sections use the solution model of Holland and Powell (1998). P-T pseudo-sections have been build in the system Na_2O, CaO, MgO, K_2O, SiO_2, Al_2O_3 and FeO, taking into account the whole rock composition and mixing models for metamorphic assemblages.

The chlorite-phengite pair (Vidal and Parra, 2000) is used to constrain P-T conditions of D1 and D2 structures. Such a method is especially suitable because the equilibration of these minerals in wide P-T ranges is mostly achieved by crystallization and recrystallization processes. We estimate P-T conditions of high-variance parageneses with multi-equilibrium calculations taking into account the composition of phases end members and calculated the P-T position of these reactions using TWEEK software (Berman, 1991) in association with the JUN92 database. This provides thermodynamic properties for Mg-amesite, Mg-sudoite, Mg-celadonite, and chlorite together with mica solid-solution models from Vidal et al. (1992, 1999, 2001, 2005), Vidal and Parra (2000) and Parra et al. (2002 and 2005). Because of uncertainties in analytical and thermodynamic data equilibriums calculated for a given paragenesis often did not intersect at a single point. P-T conditions were thus calculated using the INTERSX software selecting solutions having P and T uncertainties lower than 0.1 GPa and 25°C respectively.

- $^{40}Ar/^{39}Ar$ dating

Phengite were dated by the step heating $^{40}Ar/^{39}Ar$ technique. For each sample (M80, M173 and M196), micas along the main foliation were separated according to their size and then dated. Mineral separation has been realized using sieves and magnetic separation methods and finally hand picking under binocular control in order to exclude mixed, kinked and/or altered grains. The samples were irradiated at the McMaster University reactor, Ontario, in the 5C position for 40 h. under a 10^{18} neutrons $cm^{-2}s^{-1}$ flux from January 17th to January 19th 2005. Irradiation interference by K, Ca and Cl were corrected by irradiating pure

KCl and CaF_2. J factor was estimated by the use of duplicates of the Fish Canyon sanidine standard with an age of 28.48 Ma (Schmitz and Bowring, 2001; Schmitz and al., 2003). The samples were analyzed at the University of Montpellier. Samples were loaded in Al packets into a double vacuum Staudacher-type furnace, which was heated following the procedure described in Arnaud et al. (2003) and the temperature of which was monitored using a thermocouple.

3. Structure of the Modane-Aussois and Southern Vanoise units

- D1: nappe stacking and duplex formation

In the Modane-Aussois unit, the expression of the D1 deformation slightly differs from the Clarea and Ambin Groups to the cover. Clarea and Ambin Groups present relics of D1 folds at various scales in the field and along borehole (Figures 4B and 7B). The original large-scale geometry of the D1 folds is difficult to access because of later deformation phases. However, correlation between boreholes on the eastern part of the section C-D (Figure 6B), suggests that at least three recumbent and isoclinal hectometre-scale D1 folds lay in the prolongation of thrusts within the Briançonnais cover.

At the surface, white quartzite are the most abundant rocks of the Modane-Aussois area despite their relative small thickness (Figure 5). This is due to the duplication of white quartzite slices by at least four D1 thrust sheets. These thrusts bring thin layers of the Etache, Ambin and per place Clarea groups over decametre thick middle Triassic carbonates and/or directly over the white quartzites (Figures 5, 6B). In most places, the sedimentary bedding within the white quartzite is parallel with the thrust plane suggesting kilometre scale displacement along thrust flats (figure 6A & B). D1 folds related to thrusts are locally preserved (Figure 5). The thrust roots are characterised by a progressive thickening of the overthrusting Etache, Ambin and Clarea units that progressively evolve as isoclinal D1 folds. This strongly suggests that micaschists from Ambin and Clarea units act as a décollement layer controlling a thin skin tectonics at the scale of the Modane-Aussois unit (Figure 5). Most D1 thrusts root to the east or SE in the siliceous unit suggesting that the deformation is controlled by top to the west or NW directions of shearing. Over the siliceous duplex, the D1 deformation of Esseillon carbonates is characterized by isoclinal and recumbent folds underlined by dolomite rich strata with axes oriented N160-30°S.

The initial geometry of the L1 lineations in the Modane-Aussois unit can be estimated by taking into account D2 folding and late tilting (see below) (Figure 8a and table 1). After variable unfolding along N30° and N90° axes the unfolded L1 lineations trend between N90 and N160 and dip to the SE. This geometry is compatible with a top to the NW direction of shearing.

In the Southern Vanoise unit, Clarea and Ambin groups are affected by isoclinal folds underlined by relic of layering (Figure 4E). As already mentioned by Ganne et al., (2005), and Gerber (2008), the Clarea-Ambin group boundary displays D1 folds both at the outcrop (Figure 4F) and map (Figure 5) scales. D1 foliations dip either to the NW or the SE due to D2 folding with a N30 trending axe (Figure 8E). After unfolding around this axe, the N160-60°SE trending lineation of sample M278 is sub-horizontal and trends NW-SE.

D1 deformations present several similarities in the Modane-Aussois and Southern Vanoise units: In the Clarea and Ambin groups, it corresponds to isoclinal folds associated with a D1 foliation which orientations may vary because of later tectonic phases. In the Modane-Aussois unit, we propose that D1 folds are recumbent folds forming the roots of the white quartzite slices. Within the Southern Vanoise unit, the D1 recumbent folds have been affected by later deformation phases. In preserved area, the stretching lineation is oriented

NW-SE. Whilst no shearing criteria have been found within the Southern Vanoise unit, we propose a similar top to the NW direction of shearing for the D1 deformation phases in the Modane-Aussois unit.

- *D2: Top to the ESE and SE deformations*

Within the Modane-Aussois unit, D2 deformations within the Clarea, Ambin and Etache groups have been recognized along boreholes (Figure 7), on each side of the Arc Canyon (Figure 5 and 6B) and on the eastern flank of the Rateau d'Aussois (Figure 4C). It is characterized by a relatively flat lying foliation mostly dipping to the W (Figure 8D). C/S structures indicate a top to the E sense of shearing (Figure 4C). At the outcrop scale, D2 deformation results in the folding of the earlier structures such as he bedding and D1 folds and thrusts figure 4D). Where D2 deformation is milder, D1 recumbent folds are only affected by numerous small D2 structures forming asymmetric folds compatible with a top to the east direction of shearing, as for example on the eastern part of the CD cross section (Figure 6B). This can be observed at the surface along the Arc canyon section where a D1 tectonic contact is back-folded and sheared by several meter-scale asymmetric D2 folds.

West of the studied area, the kilometre-scale "Bourget Roc" anticline and syncline affect the D1 quartzite slices (Figure 6B). The hinges of the folds trend N18-21°S (Figure 8C), the axial planes dip to the W with an overturned eastern limb, implying an E-SE vergence. The core of the anticline consists of a complex association of Ambin group and Loutraz conglomerates probably due to folding during the D1 phase. To the North, the western limb of the anticline corresponds to the "Râteau d'Aussois shear zone" (Figure 5 and 6A), that is a 100 meters thick mylonite zone along which the Ambin group and Loutraz conglomerates of the Modane-Aussois unit are thrust over the Southern Vanoise unit. The shear zone roots to the west in the Modane-Aussois unit basement (Figure 5). As both the "Bourget Roc" and the Râteau d'Aussois shear zone affect D1 structures they are related to the D2 phase.

At the top of the Arc canyon section, the contact between the white quartzite and the Esseillon group corresponds to a 4 meters thick mylonite (Figure 6B). Within the mylonite, two phengite-bearing foliations are distinguished. The first one, associated with a N125° lineation and the top to the west shear criteria, is compatible with D1 deformation. This first foliation is folded and a new foliation orientated N165-30° E is associated with top to the east C-S microstructures compatible with D2 deformations. This shear zone is also observed farther east along the Avrieux borehole where it is responsible for apparent thinning of the series as no quartzite layers are found between the mid-Triassic mudstones and the Etache group (Figure 6B). Because the Arc canyon shear zone is not affected by meter scales asymmetric D2 folds observed near the Arc river, we propose that the Arc canyon shear zone formed at the end of the D2 tectonic phase and roots to the east (Figure 6B).

Within the Southern Vanoise unit, D2 foliations are widely expressed within the Clarea, Ambin and Etache units where a second foliation forms the axial plane of fold affecting the D1 foliation (Figure 4F).

Most D2 foliation planes dip gently to the northwest (Figure 8D and 8F) and D2 fold axes trend NE-SW (Figure 8 C, D, E), suggesting that D2 folds are recumbent. When observed, the D2 phengite-bearing lineation trends N090° to N120°. Near the top of the Southern Vanoise unit, the strong D2 deformation transposes all previous structures (Figure 6A). This relatively flat shear zone is on the prolongation of a structure already described northward (Debelmas et al., 1989, Ganne et al., 2005, Gerber 2008). The root of this structure is difficult to access as the shear zone is hidden by the Briançonnais cover on their eastern and western prolongations leaving open the possibility that it could be either a reverse shear zone

rooting to the west or a detachment rooting eastward. The contact between the Southern Vanoise unit and the Modane-Aussois unit is underlined by the Râteau d'Aussois shear zone that puts the Modane-Aussois unit over the Southern Vanoise unit. Thus this relative position of these two units is achieved during the D2 deformation phase and there is no evidence that that was the case prior the top to the E deformation phase.

- *Late tiltings.*

On the northern side of the Arc valley, the D2 folds (Figure 8C), the bedding plane in the quartzites and the tectonic sole of the Dent Parrachée unit form a structural surface roughly parallel to the topography, dipping about 20-30° toward the south. The D2 fold axe within the Rateau d'Aussois shear zone and the sole of the Dent Parrachée unit drop by 1400 m of the altitude from north to south. We interpret this geometry as resulting from a late southward tilting around an east-west axis of the whole area (D3). The highest structural units outcrop in the south of the area on the southern side of the Maurienne valley in good agreement with this tilting (Figure 2 and 5).

4. Micro structures and mineral chemistry

D1 and D2 deformation phases are associated with different mineral assemblages . Rocks from the Clarea group show glaucophane and white mica crystallising along the D1 foliation both in the Southern Vanoise and the Modane-Aussois units (Figure 9A, B and C and Figure 10). Garnet is only present in the Southern Vanoise unit (Figure 9A and Figure 10). Within the Ambin group, the D1 foliation is underlined by chlorite and white mica in the Modane-Aussois and the Southern Vanoise units (Figure 9D). In the Etache and the white quartzites groups of the Modane-Aussois unit, white mica underlines the D1 foliation (Figure 9).

Everywhere in the studied area, D2 structures are underlined by white mica, albite and chlorite (Figure 9 A, B, C, 10 and 11) and in the case of the Clarea group of the Modane-Aussois unit by a second generation of glaucophane (Figure 9B).

Thus in most case, no index mineral can be directly used in order to decipher the D1 and D2 foliations. Only relative chronology between both foliations and the textural relationship between albite and the foliation is helpful as albite crystallizes everywhere after D1 foliation (Figures 9 and 11). In the following section, we present the chemical properties of the main metamorphic mineral of the studied area.

- *Garnet*

Garnets do not exceed 200µm in size (Figure 9A and 10) and are only found in the Clarea group of the Southern Vanoise unit. They have a rounded shape indicating a possible destabilization. They are located along the D1 foliation and are per place included within glaucophane, suggesting that the growth of some glaucophane grains occurred after the growth of the garnet (Figure 9A). Garnets contain few Inclusions and are a solid solution of almandine (X_{Alm} = 0.65 – 0.75), grossular (X_{Grs} = 0.22 – 0.27), pyrope (X_{Py} = 0.03 – 0.05) with a minor spessartine component (X_{sps} = 0.01 – 0.05) (Table 2 and Figure 12A). The only chemical variation observed within the garnets is an increase of X_{Fe} at the rims and near the fractures (Figure 12A). Following Ganne et al. (2003), we interpret this as the consequence of diffusion processes during late exhumation of the Clarea micaschists. Garnets in the Brianconnais basement have been described in the Southern Vanoise unit farther to the east (Ganne et al., 2003 and reference therein). On the basis of the link between mineral inclusions

(glaucophane + phengite versus biotite and muscovite), Ganne et al. (2003) have proposed that the growth of Mn rich garnets is related to pre-alpine metamorphism whereas Mn Poor garnets grow during alpine metamorphism. When projected on a Fe+Mg, Ca, Mn plot, chemical analyses of the Clarea group garnets (Figure 12A) are in field of alpine garnet.

- *Phengite*

Phengite is abundant in every unit. The mineral underlines both D1 and D2 foliations. Its size range between less than 50 up to 300µm, with those associated to D2 being generally smaller than those associated to D1. Phengites are a solid solution between muscovite (Xmu = 0.5 – 0.95), celadonite (Xcel = 0.05 – 0.45) and pyrophilite (Xpyr = 0 – 0.5) (Table 2). Within the Clarea and Ambin groups, a significant component of paragonite is observed in several phengites. Si rich phengites have a minor paragonite component relative to lower Si phengites (Figure 12B and D). As there is few evolution of the Si content in the phengites from the Brianconnais cover, no enrichment on paragonite content has been observed (Figure 12 C).

In the Clarea and Ambin groups of the Southern Vanoise and Modane-Aussois units, three main groups of white mica are distinguished. Group 1 consists of nearly pure muscovite that are found both along D1 and D2 foliations (Figure 10, 11) and have low Si content < 3.15 p.f.u. (Figure 12B and D). Group 2 is characterized by phengites with a large amount of celadonite (Xcel >0.3), with Si content greater than 3.35 p.f.u. (Figure 12B and D), that are observed both along the D1 and D2 foliations (Figure 10 and 11). Group 3 corresponds to phengite with an intermediate composition between groups 1 and 2 (Xcel = 0.15 – 0.3) having a Si content ranging between 3.1 and 3.3 p.f.u. (Figure 12B and D), that are mostly located along D2 structures (Figure 10 and 11). In agreement with previous studies on the Briançonnais domain (Ganne et al., 2003, Gerber et al., 2008 and reference therein), we propose that the group 1 corresponds to pre-alpine muscovite formed under amphibolite facies metamorphism, the group 2 corresponds to alpine phengites that crystallized during the HP-LT event associated with D1 structures and the group 3 corresponds to phengites that have crystallized during the exhumation of HP-LT rocks during the D2 phase (Figure 12B and D). The large amount of phengites from the group 1 found along D1 and D2 structures, and of group 2 phengites found along D2 structures suggest that both mechanical re-orientation and crystallization of new phengites occurred during each alpine phases (Figure 10 and 11)

In the Brianconnais cover, the use of phengite chemistry to decipher between D1 and D2 tectonic events is not useful as there are no direct relationships between structural site and Si content of phengite (Figure 12C). At the sample scale, D1 and D2 phengites have in most samples the same chemical composition. As it is the case of basement rocks, we also recognized phengites underlining D2 structures with Si content greater that 3.3 p.f.u. This observation is compatible with the previously proposed explanation of mechanical re-orientation of D1 phengites along D2 structures. However, within sample MO196, the fact that D2 phengites are bigger than D1 ones strongly suggest that D2 phengites with Si content greater that 3.3 can also crystallize later (Figure 12C). This implies that in the case of the Brianconnais cover where highly siliceous rocks such as quartzite are abundant, the whole rocks composition may play a more important role than the P-T conditions on the chemical composition of phengite.

- *Chlorite*

Chlorite is abundant within the Clarea and Ambin units and rare or absent within the Brianconnais cover (Figure 9). Within the Ambin group, chlorite underlines both D1 and D2 structures in association with phengite. In that case, the contact between these two minerals

follows the foliation (Figure 9). In the Clarea Group of the Southern Vanoise unit, chlorite is found along D2 structures and around glaucophane and garnet (Figure 9 and 10). In this later case, chlorites can either be crystallized during the end of the D1 or during de D2 tectonic phase. Chlorites are a solid solution between clinochlore + daphnite (Xclin+daph = 0.28-0.72), sudoite (X sud = 0 – 0.25) and amesite (Xame = 0.2 - 0.36) suggesting a wide range of chemical composition. Within the Clarea group, chlorites that grow around garnet and glaucophane have a similar composition with chlorites located along D2 structure (Table 2). This suggests that all the chlorite of the Clarea group crystallize during the D2 event.

- *Glaucophane*

Glaucophane is only present in the Clarea group, both in the Southern Vanoise and in the Modane-Aussois units (Figure 9). Within the Southern Vanoise unit, minerals are up to 1mm long with a sub-automorph shape and are elongated within the D1 foliation. These Glaucophanes contain per place garnet, phengite and zircon as inclusions and are frequently surrounded by chlorite, phengite and biotite. We propose that these glaucophanes crystallize during D1 deformation while the formation of chlorite, phengite and biotite around them occurred possibly at the end of the D1 of during the D2 tectonic phase (Figure 9 and 10). Per place, we recognized also small automorph and fresh glaucophane following D2 orientation (Figure 9). There is no chemical change between D1 and D2 elongated glaucophane. Two hypotheses can explain the occurrence of glaucophane along the D2 foliation: glaucophane could crystallize during D1 deformations are be re-orientated along the D2 foliation, or some glaucophanes may also crystallize during the D2 tectonic event. The second interpretation would better explain the good preservation of glaucophane minerals found in D2 structures.

5. Pressure and temperature conditions of the deformation phases

P-T estimates were performed on samples both from the Modane-Aussois unit: glaucophane bearing micaschist (M266 sample) and chlorite bearing micaschists (F21-5, M290, M259 samples), and from the Southern Vanoise unit (M278 sample).

Sample M266 is located on the sole of a D1 thrust within the Briançonnais cover (Figure. 5). It is a dark micaschist that has been interpreted as belonging to a slice of the Clarea group pinched on the sole of a D1 trust duplicating the white quartzite layer (Figure. 5). Two foliations have been observed: the earlier (D1) is underlined by glaucophane and is re-folded. The second foliation, underlined by chlorite, forms the axial plane of he folds and has been attributed to the D2 phase. This is the only observation of glaucophane within the Briançonnais cover duplexes.

Samples F21-5, M290 and M259 are pale micaschists from the Ambin unit (Figure 5). They characterized by the absence of glaucophane and two foliations each underlined by chlorite and phengite that belongs to D2 shear zones sampled both in borehole (sample F21-5, Figure 9D) and in the Rateau d'Aussois shear zone (sample M259 and M290, Figure 11).

M278 sample comes from the Clarea group of the Southern Vanoise unit (Figure 5). It is a micaschist showing two foliations (Figure 9A and 10). The second foliation, underlined by chlorite, is sub-horizontal and marks the axial planes of folds affecting the first one. It has been attributed to the D2 event. The first foliation (D1) is sub-vertical and underlined by glaucophane.

Pseudosection calculation assumes that the rock is fully equilibrated for each P-T condition. This assumption is probably inadequate for the whole metamorphic history as two metamorphic stages associated with D1 and D2 are observed in each sample. However, full equilibration has been probably achieved during the D1 stage, allowing the use of

pseudosections for estimating P-T conditions for this event, together with chlorite-phengite pairs when possible. On the other hand only chlorite-phengite pairs where used to characterise P-T conditions of the D2 event.

- P-T conditions of the D1 event

Pseudosection analysis of the D1 paragnesis of sample M266, containing glaucophane and phengite with Si contents between 3.4 and 3.45 p.f.u, yields P greater than 0.8 GPa and T lower than 400°C (Figure 12B, 13A). In the absence of jadeite and garnet, the stability domain has an elongated shape between 250° and 0.8 GPa and 400°C and 1.2 GPa. This pseudo section predicts the absence of chlorite, which is compatible with the growth of chlorite only during D2 within this rock (Figure 9B).

In the chlorite bearing micaschist F21-5 of the Modane-Aussois unit, D1 structures are underlined by chlorite and phengite with Si content between 3.35 and 3.45 (Figure 12B). Glaucophane and garnet have not been observed (Figure 9D). In the pseudosection, the stability field of the D1 mineral assemblage does not provide precise P-T conditions as pressure ranges between 0.5 and 1.5 GPa and temperature ranges between 300 and 500°C (Figure 13B). To better constrain the P-T conditions of D1, we conduced P-T estimate on a D1 chlorite-phengite pair. Results suggest pressure ranging between 0.9 and 0.65 GPa and T of about 350 °C (Figure 13B).

Within the Southern Vanoise unit, the D1 metamorphic assemblage is characterized by the association of alpine garnet, glaucophane, paragonite and phengite with Si content between 3.4 and 3.5 (Figure 9A, 10, 12A and 12D). On the pseudosection of sample M278, minimum P and T for the D1 assemblage are of 1.75 GPa and 470°C (Figure 13C). At these conditions, pseudosection indicates the following volumic composition: phengite (27%), Glaucophane (25%), Paragonite (14%), Garnet (2.5%) and Quartz (31.5%).

- P-T conditions of the D2 event

The glaucophane bearing micaschist of the Modane-Aussois unit (M266), yields three chlorite-phengite P-T estimates for the D2 foliation between 0.7 ± 0.1 GPa and 300 ± 30°C (Figure 13A).

Within sample F21-5, M290 and M259, D2 structures are underlined by chlorite, phengite, biotite and albite (Figure 9D). Calcite is abundant and represents the only phase containing CaO. A high CO_2 pressure may explain the absence of lawsonite, zoisite and clinozoite. We obtain 11 estimations of P-T conditions of chlorite phengite pairs. Estimates on D2 chlorite phengite pairs span between 350 °C and 0.65 GPa and 220 °C and 0.15 GPa (Figure 13B). There is no significant variation in the P and T estimates between samples F21-5, M290 and M259 suggesting that the D2 structures shear zones were active under similar metamorphic conditions everywhere in the Modane-Aussois unit.

Within the Southern Vanoise unit, phengite with Si content lower than 3.4 (Figure 12D) and Albite are the most abundant mineral phases that crystallize during the D2 deformation (Figure 9A). In addition, chlorite is also observed. Per place, glaucophane follows also the D2 foliation. 14 of the 15 analyses performed on chlorite and phengite underlining the D2 foliation of sample M278 range between 0.5±0.1 and 1.05±0.1 GPa and 260±30 and 360±30°C (Figure 13C). Highest pressures are associated with temperature around 300°C and the highest temperatures are obtained for pressure at around 0.6 GPa suggesting a slight heating during exhumation. Within this sample, early garnets are replaced by the association of chlorite, white mica and epidote (Figure 10). Textural position suggests that these chlorite and phengite pairs possibly crystallized before the formation of D2

foliation. 7 P-T estimates performed on such chlorite-phengite pairs range between 0.7 ± 0.1 and 10.5 ± 0.1 GPa and 260 ± 30°C and 370 ± 30°C (Figure 13C). These estimates are close to the one from the D2 foliation but tend to show higher pressures. This suggests that the destabilization of garnet may be coeval with the onset of D2 deformation and continues later.

- *P-T-d paths*

The P-T-d paths of all samples from the Modane-Aussois unit, containing glaucophane or not, are characterized by an isothermal exhumation at 350°C ± 30° from 1.0 ± 0.1 GPa to 0.3 ± 0.1 GPa, followed by a decrease of both P and T close to surface conditions (Figure 13 A and B). Peak metamorphic conditions and the beginning of exhumation are associated with the D1 deformation phase. The chlorite-phengite pairs constrain the transition to the D2 deformation to occur around 0.75 ± 0.1 GPa and 350 ± 30°C. M266 glaucophane bearing micaschist of the Modane-Aussois unit exhibits a small automorph glaucophane that crystallized during D2 event. This is in contradiction with M266 pseudosection where glaucophane is absent at ~0.75 GPa and ~350°C. This suggests either that the glaucophane was re-oriented during D2 or that the pseudosection does not represent the correct stability fields at the D1-D2 transition because of chemical disequilibria. The D1-D2 transition is associated with albite and chlorite crystallization. Such minerals are present in the pseudosection at pressure below 0.8 GPa. P-T conditions below 0.8 GPa and at T = 350 ± 30°C are also recorded by chlorite-phengite pairs in sample F21-5. We thus suggest that D2 deformation started during the exhumation at ~0.75 GPa and ~350°C and lasted until 0.2±0.1 GPa and 280±30°C (Figure 13B).

Analyses within sample M278 suggest similar or slightly greater conditions for the D1/D2 transition (0.7 to 10.5 GPa and 370 ± 30°C) in the Southern Vanoise unit (Figure 13C) than in the Modane-Aussois unit (Figure 13A, B). A single D2 chlorite-phengite pair suggests that the end of the exhumation path may also be similar (Figure 13B, C). P-T estimates for D1 are indicate a much higher pressure in the Southern Vanoise unit at 1.75 GPa and 470°C (Figure 13C).

6. Geochronological constraints on the Modane-Aussois Unit

Three samples have been selected for dating: M80, M173 and M196 (Figure 5). It has been demonstrated that there is a relationship between the paragonite component of phengite and the ^{39}Ar excess (Gerber, 2008). To avoid ^{39}Ar excess problem, we only selected phengites from samples of the Brianconnais cover that are characterized by the absence of paragonite component (Figure 12). Classical step heating was performed and plateau ages were calculated. Very little ^{36}Ar has been extracted, precluding the use of isochron ages.

Interpretation of radiometric age is always faced with the problem of closure temperature of the isotopic system. In the case of the ^{40}Ar/^{39}Ar method on white micas, closure temperature range between 350 and 450°C (McDougall and Harrison, 1988). As the studied white micas crystallized at a maximum temperature of ca. 350°C we consider that mica ages represent crystallization ages and allow to directly date deformation phases (Figure 13).

- *dating the D1 event (Sample M80)*

M80 is a Permo-Triassic sample located at the base of a D1 quartzite thrust sheet (Figures 5 and 6). The sample is composed of quartz, dolomite and phengite. It is affected by an intense D1 foliation underlined by phengite (125 to 250 µm. in size) (Figure. 14A). At the

microscopic scale, small size (< 10µm) white micas are observed, these grains do not follow de D1 foliation and are possibly inherited grains. The narrow range of phengite contents, between 3.25 and 3.35 Si p.f.u., suggests a single population (Table 2 and Figure 12C).

^{40}Ar /^{39}Ar spectrum is characterized by a saddle shape. A weighed average age of 37.12 ± 0.39 Ma is calculated between 17 and 92% of ^{39}Ar released (75% of ^{39}Ar released) (Figure 14J). These steps are associated with high K/Ca and low Cl/K ratios suggesting a rather homogeneous white micas source of all steps (Figure 14D and G). A slight component of excess Ar might exist because of the saddle shape (first and last steps at 40.53 ± 0.13 Ma, Figure 14J), This is confirmed by an increase of the Cl/K ratios (Figure 14D). Inverse isochron can be hardly calculated in this case due to the scattering of data. Alternatively, coupling between ages and K/Ca ratios may be related to the contribution of a small amount of inherited micas (Figure 14G).

The weighed average age is constrained by three steep, more than 70% of ^{39}Ar released and because low K/Ca and high Cl/K ratios for these steps are constant, we consider that the 37.12±0.39 Ma age is reliable and represent the D1 event.

- *dating the D2 event (Samples M173and M196)*

M173 has been sampled from quartzite in the hinge of the "Bourget Roc" syncline that is related to the D2 tectonic phase (Figure 5). The sample is composed of quartz and phengite. D2 foliation, lying at high angle to the stratification, is underlined by phengites (Figure 14B). The orientation of the foliation is consistent with the orientation of the axial plane of the syncline. The phengite sizes are variable; phengites defining the foliation are about 125 to 250 µm in size (Figure 14B). The sample also contain abundant small phengites (< 10µm) that were not selected for dating. Si content of M173 phengites is comprised between 3.22 and 3.32 p.f.u. (Table 2 and Figure 12C) and suggests a relatively homogeneous population.

Results are characterized by an increasing age spectra which is clearly two folds (Figure 14K): after high ages correlated probably with excess argon, ages as low as ca 25 Ma are recorded, followed by a rise of ages to a flatter portion between 38 and 98% of ^{39}Ar released. A weighed age of 35.42 ± 0.38 Ma is calculated on more than 58 % of ^{39}Ar released on the highest part of the spectra (Figure 14K). It is associated with high K/Ca and low Cl/K ratios suggesting a homogeneous white micas source for all steps (Figure 14E and H). Younger ages at the beginning of the spectrum (between 22.89 ± 0.08 and 33.08 ± 0.11 Ma) are associated with low K/Ca ratios, suggesting chemical heterogeneity possibly due to alteration of the sample or at least mixing between grains of different generations (Figure 14H). The first and the lasts steps are give older ages associated with a strong decrease of K/Ca ratios suggesting that a slight component of excess Ar might exist. The inverse isochron cannot be used due to the scattering of points along the X axis.

Because the 35.42 ± 0.38 Ma age is constrained on less than 70% of ^{39}Ar released, it is not robust. However, more than half of the 39Ar released along three consecutive steps presents similar characteristics: low K/Ca and high Cl/K ratios and similar age (Figure 14E and H). This suggests that even if the sample is affected by slight component of excess Ar and a possible alteration or re-crystallization of the white micas a part of the spectrum corresponding to circa 35-36 Ma dating is representative of the D2 tectonic event although this age is rather close to the D1 age.

Sample M196 was collected from a strongly deformed quartzite, within the D2 contact between carbonate and the quartzite in the Arc canyon (Figures 5 and 6). The sample is composed of quartz, dolomite, calcite and white micas. Two phengite generations are recognized. The first generation shows small grains, < 50µm in size, along the first foliation

that is strongly transposed by the second tectonic phase (Figure 14C). The second generation of phengite is associated with folding and occurs along a new foliation parallel to the fold axial planes of the D2 event. Phengite crystallized during the second event is larger (125 – 205µm in size) and can be easily distinguished from the earliest phengite. The Si content of M193 phengites varies between 3.3 and 3.35 p.f.u. (Table 2 and Figure 12C).

The ^{40}Ar /^{39}Ar spectrum is complex, but a 31.60 ± 0.33 Ma plateau age is calculated on three steps between 21 and 98% of ^{39}Ar released corresponding to 75% of ^{39}Ar released (Figure. 14L). It is associated with constant high K/Ca and low Cl/K ratios suggesting a homogeneous white micas source for all steps (Figure. 14F and I). Between 11% and 21% of ^{39}Ar release, the spectrum is characterized by younger ages between 24.99 ± 0.9 and 28.81 ± 0.08 Ma and is associated with a decrease of K/Ca and an increase of Cl/K ratios. This suggests chemical heterogeneity of the sample possibly due to re-crystallization of a part of the phengites. The first and the lasts steps are associated with older ages associated with a strong decrease of K/Ca ratios suggesting that a slight component of excess Ar might exist (Figure. 14I and L). No useful inverse isochron can be built from the data.

Because the plateau age is constrained by three steep, more than 70% of ^{39}Ar released and because low K/Ca and high Cl/K ratios for these steps are constant, we consider that the 31.60 ± 0.33 Ma age is reliable and represent the D2 event, and is probably more reliable than the age from sample M173 which might be intermediate and mixed between D1 and D2.

7. Discussion

The P-T conditions for D1, correspond to a geothermal gradients between 13 and 18°C km^{-1} in the Modane-Aussois unit and between 9 and 14°C km^{-1} in the Southern Vanoise unit (Figure 13). Such values are is in good agreement with those obtained in the internal Briançonnais zone (Bucher et al., 2003). This suggests that the Modane-Aussois unit and the Southern Vanoise units where buried in a similar context as the rest of the Briançonnais zone.

In the following discussion, we build a P-T-t-d path for the Modane-Aussois and Southern Vanoise units and then, we discuss the signification of the D2 tectonic phase and the possibility of a thrusting of the Southern Vanoise unit on the Modane-Aussois unit during the D1 tectonic phase. Finally, we discuss the processes that led to the exhumation of the Brianconnais zone.

- P-T-t-d path of Modane-Aussois unit

The P-T path of the Modane-Aussois unit is characterized by an isothermal exhumation at 350 ± 30° between 1.0 ± 0.1 GPa and 0.3 ± 0.1 GPa followed by a decrease of both P and T up to surface conditions (Figure 13A, B). Maximum metamorphic conditions and the beginning of exhumation are associated with the D1 deformation phase. The age of 37.12±0.39 Ma obtained on M80 phengites thus probably reflects the early stage of exhumation. Transition between D1 and D2 deformation phases took place at ~0.8GPa and ~350°C. Then, D2 deformation continued until 0.2 ± 0.1 GPa and 280 ± 30°C (Figure 14). The phengites of sample M173 and M196 have crystallized during the early and late stages of D2 respectively. Their respective ages would thus imply that D2 deformation started around 35 Ma ago and lasted until at least 31.60±0.33 Ma.

- P-T-t-d path of Southern Vanoise unit

In the absence of new geochronological data, age constraints for the South Vanoise P-T-d-t path come from $^{40}Ar/^{39}Ar$ and $^{87}Rb/^{86}Sr$ data from the literature (Ganne 2003, 2007,

Gerber, 2008). Such data show a large spread in age and are difficult to interpret because of multiple phengite generations, metamorphic peak temperature above the phengite closure temperature and excess Argon (Ganne 2003, Gerber, 2008). Samples containing paragonites attributed to D1 foliation yield very old ages (264 -103 Ma) obviously affected by excess argon (Gerber, 2008). The only D1 dated phengites devoid of paragonite are found in the Ambin unit farther to the east (samples WVS05.53 and WVS05.55B) and yield ages between 80 and 50 Ma (Gerber, 2008). Because these ages were obtained by $^{40}Ar/^{39}Ar$ laser ablation, they could be affected by Ar excess and should be considered as maximum ages. Gerber (2008) proposes an age of ~50 Ma for D1. D1-D2 and D2 phengites from five samples of the Southern Vanoise have been analyzed, yielding ages between 49 and 28 Ma (Gerber, 2008). This led Gerber (2008) to propose that D2 started at ~43 Ma, and that eastward shear took place between 37 and 28 Ma, with a climax at ~34 Ma. Ganne et al. (2007) suggest an age of 35Ma for D2 in the Ambin unit, based on $^{87}Rb/^{86}Sr$ data. These data are compatible with an age of ~37 to ~28 Ma for D2, close to the age we propose within the Modane-Aussois unit. The age of D1 is less well constrained. It may have started at ~50 Ma and lasted until 48 or 37 Ma depending on how the ages of D1-D2 phengites are interpreted.

We suggest that D2 took place from ~37 to ~28 Ma both in the Modane-Aussois and South Vanoise units. In the Southern Vanoise Unit, D1 occured during exhumation from 1.75 GPa to 10.5 GPa, cooling between 470°C and 370°, possibly starting at ~50 Ma and lasting until ~37 Ma. D1-D2 tansition takes place around 0.7 to 10.5 GPa and 370 ± 30°C at ~37Ma, while D2 deformations last until 0.2±0.1 GPa, 280±30°C at~ 28 Ma.

- *Metamorphic gap and the origin of the contact between Modane-Aussois unit and Southern Vanoise unit*

Changes in mineral assemblages imply a significant P and T increase from the Modane-Aussois unit to the Southern Vanoise unit. Our results confirm the occurrence of a metamorphic gap between the two units as already suggested by several authors (Oberhänsli et al., 2004, Ganne et al., 2005, Strzerzynski, 2006 and Gerber, 2008). We estimate this gap at 0.6 ± 0.3 GPa and 150 ± 130°C (Figure 15B). The Modane-Aussois and Southern Vanoise units are separated by a D2 shear zone suggesting that the D2 tectonic phase is responsible for the final emplacement of the Modane-Aussois unit against the Southern Vanoise unit (Figure 15A). However, at the onset of D2 (~37 Ma) P-T conditions in the two units were relatively close to each other (Figure 15C). This suggests that the metamorphic gap was reduced during the D1 tectonic phase (Figure 15C), possibly via a thrust bringing the Southern Vanoise unit from greater depth to on top of the Modane-Aussois unit (Figure 15A). Structural evidences for this thrust may have been erased by D2 overprint.

The hypothesis of a major D1 thrust between the Southern Vanoise and Modane-Aussois units is supported by other lines or argument:

(1) The abundant mesozoic syn-rift sedimentary series of the Southern Vanoise unit (Dent Parrachée unit) are absent from the Modane-Aussois unit (Figure 3) suggesting distinct paleogegraphic origins.

(2) Peak temperature of 420°C ± 50°C for the Dent Parrachée unit (Gabalda et al., 2008) are close to the temperature estimates in the Southern Vanoise but significantly higher than those of the Modane-Aussois unit suggesting that that the two former units share a common early history contrasting with that of the Modane-Aussois Unit.

(3) The Modane-Aussois unit appear structurally above the Southern Vanoise and Dent Parrachée units only in the reversed western limb of a syncline located in the footwall of a D2 top to the East shear zone (Figure 6A and B). Considering this, the Southern Vanoise unit was structurally above the Modane-Aussois unit and D1 contact between the Modane-Aussois and

the Southern Vanoise Units was probably flat before being steepened during the D2 deformation phase. This scenario is compatible similar observations and interpretations of deformation within the Southern Vanoise Unit (Ganne et al., 2005; Gerber, 2008; this study).

We propose that the D1 deformation phase accommodated exhumation of the Southern Vanoise unit until the D1-D2 transition (Figure 15) at ~38 Ma. The thrust contact was overprinted by later top to the east D2 deformations.

- a tectonic and metamorphic evolution of the Piedmont, Southern Vanoise and Modane-Aussois units

East of the studied area, three main phases of deformation have been recognized in the Piedmont unit (Figure 1, Agard et al., 2002). The first tectonic phase is coeval with HP metamorphism and associated with top to the north thrusting and is dated between 62 and 55 Ma. The second tectonic phase took place between 51 and 45 Ma during the exhumation of the Piedmont zone in a context of ductile extension with top to the east and SE shear zones. The third tectonic phase corresponds to the end of the exhumation and is associated with top to the west shear zones and extension.

Combining our results with the P-T and structural evolution of the Piedmont zone, we propose a four stages tectonic and metamorphic evolution for the internal Alps (table 4, Figure 15).

(1) Between 60 and 50 Ma, burial of the Piedmont zone in an oceanic subduction context (top to the NW thrusting).

(2) Between 50 and 45 Ma, burial of the continental Southern Vanoise unit and exhumation of the Piedmont zone in a context of top to the NW thrusting (Figure 16A). During this stage, pressure in the Piedmont zone becomes lower than that in the Southern Vanoise unit suggesting thrusting of the former unit on top of the later (Figure 15C). This stage corresponds to the initiation of continental subduction. At that time the Modane-Aussois unit is not yet buried.

(3) Between 45 and 37Ma, burial of the Modane-Aussois unit and exhumation of the Southern Vanoise in a context of top to the NW thrusting (D1) associated with the exhumation of the Piedmont zone in a context of top to the SE direction of extension (Figure 16B). This can be explained by extrusion tectonics of the Southern Vanoise unit as proposed by Ganne et al. (2006). During this second stage of continental subduction, the Modane-Aussois unit is not as deeply buried as the Southern Vanoise unit was in the previous stage. This suggests that the ability of the continental margin to be subduct progressively decreased probably due to a decrease of the convergent rate between Europe and Apulia (Handy et al., 2010).

(4) Between 37 and 31 Ma, top to the E direction of shearing starts to exhume the Modane-Aussois and the Southern Vanoise units in a context of top to the SE direction of shearing (Figure 16C). At the beginning of this stage, exhumation of the Piedmont zone occurred in a context of top to the W direction of extension (Agard et al., 2002). This tectonic stage is coeval with the activation of the Penninic Thrust and begining of the collision stage (Schmidt and Kissling, 2000, Pfiffner et al., 2002, Leloup et al., 2005, Rosenbaum et al., 2005, Rolland et al. 2008, Simon-Labric et al., 2009, Beltrando et al., 2010, Dumont et al., 2011).

- The signification of the top to the E tectonic phases

Even if in the internal part of the Alps structures with a top to the east shear sense have been described since a long time, their signification is still highly debated. Since at least 20

years, various models have been proposed to explain these structures: back-thrusting (Tricart, 1984; Freeman et al., 1997, Gabalda, 2008), back-folding (Bucher et al., 2003), detachment related to extension (Ganne et al., 2007, Gerber 2008). If this debate is not yet settled, this is because it is not clear whether these structures (1) root in the inner or the outer part of the belt and (2) were activated in a general context of alpine continental subduction or continental collision.

Our results suggest that the D2 top to the east shear zones roots to the west as the Râteau d'Aussois shear zone (Figures 6B, 8D and F and 15A). Our time constraint imply that D2 structures formed between 37 and 31Ma at a time of plate tectonics reorganization in the alpine domainand the activation of the Penninic front (Rolland et al. 2008, Simon-Labric et al., 2009, Handy et al., 2010 Dumont et al., 2011). This implies that D2 structures are more related to backthrusting coeval with the activation of major thrusting towards the external part of the belt that mark the end of continental subduction and the start of continental collision in the western Alps.

8 Conclusion

By combining structural analyses, metamorphic P-T estimates, ^{40}Ar /^{39}Ar dating of micas, we propose a P-T-t-d path for the alpine evolution of the Modane-Aussois and the Southern Vanoise units. The alpine tectonics is polyphased and occurred in a context of exhumation of HP rocks. For each unit, a cold geothermal gradient is obtained for the pressure peak suggesting that continental subduction is responsible of the burial of these units. The southern Vanoise unit is buried before and at greater depth than the Modane-Aussois one, and during the D1 tectonic phase the first is thrusted on top of the second. As D1 deformations within the Southern Vanoise unit are coeval with top to the East direction of extensional shearing within the Piedmont zone, we propose that extrusion tectonic driven by buoyancy forces is the main exhumation processes for the early exhumation of the Southern Vanoise unit. Because extrusion tectonic occurred during the burial of the Modane-Aussois unit, we propose that the early exhumation of the Southern Vanoise unit also takes place in a context of continental subduction.

Considering the timing of the D2 deformation phase coeval with the activation of the Penninic Thrust, the growth of the collision wedge and the formation of foreland basins, we propose that the end of the common exhumation path of the Southern Vanoise and the Modane-Aussois units occurred in a context of continental collision where formation of reliefs and large amount of erosion govern exhumation processes. In this context, we propose that the D2 structures of the studied units are backthrusts contributing to the thickening of the collision wedge.

The exhumation of the Brianconnais zone takes place in a crucial period of the alpine belt at the transition from continental subduction to continental collision. The end of continental subduction is underlined by a rapid decrease of both the burial depth of continental units and the importance of extrusion tectonics, whereas continental collision is here characterized by the activation of backthrusts.

Acknowledgement

This study was supported by the CNRS, the EMERGENCE program of the Rhône-Alpes region and the ANR-08-BLAN-0303-01 ERD-Alps: Erosion and Relief Development in the western Alps. We thank Mary Ford, Keiko Hattori, Patrice Rey, Benoit Saumur, Pierre Tricart, Marce Bohn, Yann Rolland and two anonymous reviewers for fruitful suggestions.

References

Agard, P., Monie, P., Jolivet, L. et Goffe, B., 2002. Exhumation of the Schistes Lustres complex; in situ laser probe 40Ar/39Ar constraints and implications for the Western Alps. Journal of Metamorphic Geology, 20, 599-618.

Agard P., Yamato P., Jolivet L., and Burov E., 2008. Discontinuous exhumation of oceanic crust: insights from blueschists and eclogites into the subduction channel. Earth Sciences Reviews, 92, 53-79.

Aillères, L. 1996. Structure et cinématique de la zone Houillère Briançonnaise entre Arc et Isère (Alpes Française) : apport de l'inversion des données de la déformation finie aux modèles cinématiques classiques. Unpublished Thesis, Nancy, 1996

Arnaud N., Tapponnier P., Roger F., Brunel M., Schärer U., Wen C., and Xu Z., 2003. Evidence for Mesozoic shear along the western Kunlun and Altyn-Tagh fault, northern Tibet (China). Journal of Geophysical Research - Solid Earth. 108.

Beltrando, M., Compagnoni, R., Lombardo, B. 2010, (Ultra-) High-pressure metamorphism and orogenesis: An Alpine perspective, Gondwana Research 18, 147-166, doi:10.1016/j.gr.2010.01.009

Berman RG., 1991. Thermobarometry using multi-equilibrium calculations: a new technique, with petrological applications. Canadian Mineralogist 29: 833-855.

Bertrand, J.-M. and Leterrier, J., 1997. Granitoides d'age Paleozoique inferieur dans le socle de Vanoise meridionale: geochronologie U-Pb du metagranite de l'Arpont (Alpes de Savoie, France). Comptes Rendus de l'Académie des Sciences - Series IIA - Earth and Planetary Science, 325, 844.

Bertrand, J., Pidgeon, R., Leterrier, J., Guillot, F., Gasquet, D. and Gattiglio, M., 2000. SHRIMP and IDTIMS U-Pb zircon ages of the pre-Alpine basement in the Internal Western Alps (Savoy and Piedmont). Schweizerische Mineralogische Und Petrographische Mitteilungen, 80, 225-248.

Bocquet, J., Delaloye, M., Hunziker, J. and Krummenacher, D., 1974. Dating of blue amphibole, micas and associated minerals from the western Alps. Contributions to Mineralogy and Petrology, 47, 7-26.

Borghi, A., Compagnoni, R. and Sandrone, R., 1999. Composite P-T paths in the internal Penninic massifs of the Western Alps; petrological constraints to their thermo-mechanical evolution. Eclogae Geologicae Helvetiae, 89, 345-367.

Bousquet, R., Goffe, B., Vidal, O., Oberhaensli, R. and Patriat, M., 2002. The tectono-metamorphic history of the Valaisan Domain from the Western to the Central Alps; new constraints on the evolution of the Alps. Geological Society of America Bulletin, 114, 207-225.

Brun, J.P., Facenna, C., 2008. Exhumation of high-pressure rocks driven by slab rollback. Earth and Planetary Science Letters, 272: 1-17.

Bucher, S., Schmid, S. M., Bousquet, R. and Fuegenschuh, B., 2003. Late-stage deformation in a collisional orogen (Western Alps); nappe refolding, back-thrusting or normal faulting? Terra Nova, 15, 109-117.

Caby, R. 1996. Low-angle extrusion of high-pressure rocks and the balance between outward and inward displacement of middle Penninic units in the Western Alps. Eclogae geol. Helv., 89,229-268.

Carrapa B. and Garcia-Castellanos D., 2005. Western Alpine back-thrusting as subsidence mechanism in the Tertiary Piedmont Basin (Western Po Plain, NW Italy) Tectonophysics 406: 197– 212

Champagnac, J.D., Delacou, B., Tricart, P., Sue, C., Burkhard, M., Allanic, C., 2006. Regional Brittle extension in Quaternary sediments of Lanslebourg (Haute-Maurienne valley, western Alps). Bulletin de la Société Géologique de France, 177, 215-223.

Chemenda AI, Mattauer M, Malavieille J and Bokun AN 1995, A mechanism for syn-collisional rock exhumation and associated normal faulting: results from physical modelling. Earth Planet Sci Lett 132: 225–232.

Chopin, C., 1987. Very high pressure metamorphism in the western Alps : implications for subduction of contiental crust. Philosophical Transactions of the Royal Society of London, A321, 183-197.

Cloos M (1982) Flow melanges: numerical modelling and geological constraints on their origin in the Franciscan subduction complex. Geol Soc Am Bull 93: 330–345.

Connoly, J. A. D., 1990. Multivariable phase diagrams: an algorithm based on generalized Thermodynamics. American Journal of Science, 290, 666-718.

de Sigoyer J., Guillot S., and Dick P., 2004. Exhumation Processes of the high-pressure low-temperature Tso Morari dome in a convergent context (eastern-Ladakh, NW-Himalaya). Tectonics Vol. 23, No. 3, TC3003 - 10.1029/2002TC001492.

Debelmas, J., Desmons, J., Ellenberger, F., Goffe´, B., Fabre, J., coll., 1989. Carte géologique de la France, feuille de Modane. BRGM (775), scale: 1/50000.

Dewey, J. F., Ryan, P. D. and Andersen, T. B., 1993. Orogenic uplift and collapse, crustal thickness, fabrics and metamorphic phases changes: the role of eclogites. Geological Society Special Publication, in Magmatic Processes and Plate tectonics, H. M. Prochard, T. Alabaster, N. B. W. Harris and C. R. Neary (Editors)

Duchene, S., BlichertToft, J., Luais, B., Telouk, P., Lardeaux, J. et Albarede, F., 1997. The Lu-Hf dating of garnets and the ages of the Alpine high-pressure metamorphism. Nature, 387, 586-589.

Dumont, T., Simont-Labric, T., Authemayou, C. and Heymes, T., 2011. Lateral termination of the north-directed Alpine orogeny and onset of westward escape in the Western Alpine arc: Structural and sedimentary evidence from the external zone. *Tectonics*, 30, TC5006, doi:10.1029/2010TC002836.

Ellenberger, F., 1958. Etude géologique du pays de Vanoise (Savoie), Mémoire Explicatif de la Carte Géologique de France, 561pp.

Ernst, W. G., 2001. Subduction, Ultrahigh-pressure metamorphism, and regurgitation of buoyant crustal slices - implications for arcs and continental growth. Physical of Earth Planetary Interior, 127, 253-275.

Escher A. and Beaumont C., 1997. Formation, burial and exhumation of basement nappes at crustal scale: a geometric model based on the Western Swiss-Italian Alps. Journal of Structural Geology, 19, 955-974.

Ford M., Duchêne S., Gasquet D., Vanderhaeghe O., 2006. Two-phase orogenic convergence in the external and internal SW Alps. Journal of the Geological Society, London, Vol. 163, 2006, pp. 1–12

Freeman, S., Inger, S., Butler, R. and Cliff, R., 1997. Dating deformation using Rb-Sr in white mica: Greenschist facies deformation ages from the Entrelor shear zone, Italian Alps. Tectonics, 16, 57-76.

Gabalda S., Jolivet L., Agard P., and Chopin C. (2008) Thermal structure of a fossil subduction wedge in the Western Alps. Terra Nova doi:10.1111:j.1365-3121.2008.00849.x.

Ganne, J., 2003. Les dômes de socles HP-BT dans le domaine Pennique des Alpes nord-occidentales (massif d'Ambin and de Vanoise Sud): modalité de leur exhumation, Ph.D. thesis, University of Savoie, Chambéry.

Ganne, J., Bertrand, J. M. and Fudral, S., 2005. Fold interference pattern at the top of basement domes and apparent vertical extrusion of HP rocks (Ambin and South Vanoise massifs, Western Alps). Journal of structural Geology, 27, 570.

949 Ganne J., Marquer D., Rosenbaum G., Bertrand J.M. and Fudral S., 2006. Partitioning of
950 deformation within a subduction channel during exhumation of high-pressure rocks: a
951 case study from the Western Alps. Journal of Structural Geology, Volume 28, 1193-1207.
952 Ganne J., Bertrand J.-M., Fudral S., Marquer D., and Vidal O., 2007. Structural and
953 metamorphic evolution of the Ambin massif (western Alps): toward a new alternative
954 exhumation model for the Briançonnais domain. Bulletin de la Société Géologique de
955 France, 178, 437-458.
956 Gay, M., 1971. Le massif d'Ambin and son cadre de schistes lustrés (Alpes - Franco-
957 italiennes). Thèse d'état, Lyon. 296p.
958 Gerber W., 2008. Evolution tectono-métamorphique du Briançonnais interne (Alpes
959 occidentales, massifs de la Vanoise et d'Ambin) : comportement du socle et de sa
960 couverture dans un contexte de subduction continentale profonde. Thèse Université Paris
961 VI, 306 p.
962 Guillot S, Hattori K, Sigoyer de J, Nägler T and Auzende A.L. 2001, Evidence of hydration of
963 the mantle wedge and its role in the exhumation of eclogites. Earth Planet Sci Lett 193:
964 115–127.
965 Guillot, S., Garzanti, E., Baratoux, D., Marquer, D., Mahéo, G. and de Sigoyer, J., 2003.
966 Reconstructing the total shortening history, of the NW Himalaya.Geochemistry
967 Geophysics Geosystems, 4(1), XXXX, doi:10.1029/ 2002GC000484.
968 Guillot S., Hattori K., Agard P., Schwartz S., and Vidal O., 2009. Exhumation processes in
969 oceanic and continental subduction contexts: a review. In S. Lallemand and F. Funiciello
970 (eds.) "Subduction Zone Dynamics", Springer-Verlag Berlin Heidelberg. doi
971 10.1007/978-3-540-87974-9, 175-204.
972 Handy, M.R., Schmid, S.M., Bousquet, R., Kissling, E., and Bernoulli, D., 2010. Reconciling
973 plate-tectonic reconstructions of Alpine Tethys with the geological-geophysical record
974 of spreading and subduction in the Alps. Earth-Science Reviews 102, 121-158. doi:
975 10.1016/j.earscirev.2010.06.002.
976 Holland, T. and Powell, R., 1998. An internally consistent thermodynamic data set for phases
977 of petrological interest. Journal of metamorphic geology, 16, 309-343.
978 Jolivet, L., Faccenna, C., Goffé, B., Burov, E. and Agard, P., 2003. Subduction Tectonics and
979 exhumation of high-pressure metamorphic rocks in the Mediterranean orogens. American
980 journal of science, 303, 353-409.
981 Lanari, P., Guillot, S., Schwartz, S., Vidal, O., Tricart, P., Riel, N. and Beyssac, O., 2011.
982 Diachronous evolution of the alpine continental subduction wedge: Evidence from P-T
983 estimates in the Briançonnais Zone houillère (France - Western Alps). *Journal of*
984 *Geodynamics*, doi:10.1016/j.jog.2011.09.006.
985 Lapen, T. J., Johnson, C. M., Baumgartner, L. P., Mahlen, N. J., Beard, B. L. et Amato, J. M.,
986 2003. Burial rates during prograde metamorphism of an ultra-high-pressure terrane: an
987 example from Lago di Cignana, western Alps, Italy. Earth and Planetary Science Letters,
988 215, 57-72.
989 Lardeaux J. M., Schwartz S., Paul A., Tricart P., Guillot S., Béthoux N., and Masson F., 2006.
990 A crustal-scale cross section of the southwestern Alps combining geophysical and
991 geological imagery. Terra Nova doi:10.1111/j.1365-3121.2006.00706x.
992 Le Bayon B. and Ballèvre M., 2006. Deformation history of a subducted continental crust
993 (Gran Paradiso, Western Alps): continuing crustal shortening during exhumation. Journal
994 of Structural Geology, 28, 793-815
995 Leloup, P., Arnaud, N., Sobel, E. et Lacassin, R., 2005. Alpine thermal and structural
996 evolution of the highest external crystalline massif: The Mont Blanc. Tectonics, 24,
997 TC4002.

998 Malusa, M., Polino, R., Zattin, M., Bigazzi, G., Martin, S. et Piana, F., 2005. Miocene to
999 Present differential exhumation in the Western Alps: Insights from fission track
1000 thermochronology. Tectonics, 24. TC3004.
1001 Markley, M. J., Teyssier, C., Cosca, M. A., Caby, R., Hunziker, J. C. and M., S., 1998. Alpine
1002 deformation 40Ar/39Ar geochronology of synkinematic white mica in the Siviez-
1003 Mischabel Nappe, western Pennine Alps, Switzerland. Tectonics 17, 407-425.
1004 McDougall, I., and Harrison, T. M., 1988, Geochronology and thermochronology by the
1005 $^{40}Ar/^{39}Ar$ method.: New York, Oxford University Press, p. 212 p.
1006 Meffan-Main, S., Cliff, R. A., Barnicoat, A. C., Lombardo, B. et Compagnoni, R., 2004. A
1007 Tertiary age for Alpine high-pressure metamorphism in the Gran Paradiso Massif,
1008 Western Alps; a Rb-Sr microsampling study. Journal of Metamorphic Geology, 22, 267-
1009 281.
1010 Megard-Galli, J. and Baud, A., 1977. The Middle and Upper Triassic of the northwestern and
1011 Western Alps; new data and stratigraphic correlation. Bull. B.R.G.M. 2° S., 4, 233-250.
1012 Oberhänsli, R., Bousquet, R., Engi, M., Goffe, B., Gosso, G., Handy, M., Koller, F.,
1013 Lardeaux, J.-M., Polino, R., Rossi, P., Schuster, R., Schwartz, S. et Spalla, M. I., 2004.
1014 Metamorphic structure of the Alps 1:1000000. CGMW, Paris.
1015 Parra, T., Vidal, O. and Agard. P., 2002. A thermodynamic model for Fe-Mg dioctahedral K
1016 white micas using data from phase-equilibrium experiments and natural pelitic
1017 assemblages. Contribution to Mineralogy and Petrology, 143: 706-732.
1018 Parra T., Vidal, O. & Theye, T. 2005. Experimental data on the Tschermak substitution in Fe-
1019 chlorites. Am. Mineral., 90, 359-370
1020 Pfiffner, O. A., F. Schlunegger, and S. J. H. Buiter, 2002. The Swiss Alps and their peripheral
1021 foreland basin: Stratigraphic response to deep crustal processes, Tectonics, 21(2), 1009,
1022 doi:10.1029/2000TC900039.
1023 Platt, J. P. and Lister, G. S., 1985. Structural history of high-pressure metamorphic rocks in
1024 the southern Vanoise Massif, French Alps, and their relation to Alpine tectonic events.
1025 Journal of Structural Geology 7, 19-35.
1026 Platt JP (1986) Dynamic of orogenic wedges and the uplift of high-pressure metamorphic
1027 rocks. Geol Soc Am Bull 97: 1037–1053.
1028 Platt, J. P., Lister, G., Cunningham, P., Weston, P., Peel, F., Baudin, T. and Dondey, H., 1989.
1029 Thrusting and backthrusting in the Briançonnais domain of the Western Alps. in Coward;
1030 Dietrich; Park (ed) Alpine Tectonics., Geological Society Special Publications. 45, 135 –
1031 152.
1032 Reddy, Wheeler and Cliff, 1999. The geometry and timing of orogenic extension: an example
1033 from the Western Italian Alps. Journal of Metamorphic Geology 17, 589.
1034 Reddy, S. M., Wheeler, J., Butler, R. W. H., Cliff, R. A., Freeman, S., Inger, S., Pickles, C.
1035 and Kelley, S. P., 2003. Kinematic reworking and exhumation within the convergent
1036 Alpine Orogen. Tectonophysics 365, 77-102.
1037 Rolland, Y., Lardeaux, J.M., Guillot, S., Nicollet, C., 2000. Extension syn-convergence,
1038 poinçonnement vertical et unités métamorphiques contrastées en bordure Ouest du Grand
1039 Paradis (Alpes Franco-Italiennes). Geodinamica Acta, 13: 133-148.
1040 Rolland, Y., Rossi, M., Cox, S.F., Corsini, M., Mancktelow, N., Pennacchioni, G.,Fornari, M.,
1041 Boullier, A.M., 2008. 40Ar/39Ar dating of syn-kinematic white mica : insights from fluid-
1042 rock reaction in low-grade shear zones (Mont Blanc Massif) and constraints on timing of
1043 deformation in the NW External Alps. In : Wibberley C.A.J., Kurtz W., Imber J.,
1044 Holdsworth R.E. & Colletini C. (eds). The Internal Structure of Fault Zones : Implications
1045 for Mechanical and Fluid-Flow Properties. Geological Society of London Special
1046 Publications 299, 293-315. DOI : 10.1144/SP299.17

1047 Rosenbaum, G., Lister, G. S. and Duboz, C., 2005. Relative motions of Africa, Iberia and
1048 Europe during Alpine orogeny. Tectonophysics 359, 117-129.
1049 Roure, F., Polino, R. et Nicolich, R., 1990. Early Neogene deformation beneath the Po Plain;
1050 constraints on the post-collisional Alpine evolution. Deep structure of the Alps, Roure;
1051 Heitzmann; Polino(editor), Mémoires de la Société Géologique de France, 156, 309-321.
1052 Schmid, S. and Kissling, E., 2000. The arc of the western Alps in the light of geophysical data
1053 on deep crustal structure. Tectonics 19, 62-85.
1054 Schmitz M. D. and Bowring S. A., 2001.-Pb zircon and titanite systematics of the Fish
1055 Canyon Tuff: an assessment of high-precision U-Pb geochronology and its application to
1056 young volcanic rocks. Geochimica and Cosmochimica Acta 65, 2571-2587.
1057 Schmitz M. D., Bowring S. A., Ludwig K. R., and Renne P. R., 2003 Comment on "Precise
1058 K-Ar, 40Ar-39Ar, Rb-Sr and U-Pb mineral ages from the 27.5 Ma Fish Canyon Tuff
1059 reference standard" by M.A. Lanphere and H. Baadsgaard. Chemical Geology 199, 277-
1060 280.
1061 Schwartz S., Lardeaux J.M., Guillot S., Tricart P., 2000. Diversité du métamorphisme
1062 éclogitique dans le massif ophiolitique du Monviso (Alpes occidentales, Italie)
1063 Geodinamica Acta. 13, 169-188.
1064 Simon-Labric, T., Y. Rolland, T. Dumont, T. Heymes, C. Authemayou, M. Corsini, M.
1065 Fornari. 2009. 40Ar/39Ar dating of Penninic Front tectonic displacement (W Alps) during
1066 the Lower Oligocene (31-34 Ma). Terra Nova, 21, 127-136.
1067 Steck A, Epard JL, Vannay JC, Hunziker J, Girard M, Moraro Aand Robyr M (1998)
1068 Geological transect across the Tso Moarari and Spiti areas: the nappe structures of the
1069 Tethys Himalaya. Eclo Geol Helv 91: 103–121.
1070 Strzerzynski, P., Guillot, S., Leloup, P. H., Ledru, P., Courrioux, G. and Darmendrail, X.,
1071 2004. Brittle deformations between the Ambin and Vanoise domes in the frame of the
1072 structural evolution of the internal Alpine belt. Virtual Explorer, 16.
1073 Sue C., Delacou B., Champagnac J., Allanic C., Tricart P., and Burkhard M. (2007)
1074 Extensional neotectonics around the bend of the Western/Central Alps: an overview.
1075 International Journal of Earth Sciences 96, 1101-1129.
1076 Thompson A, Schulmann K and Jezek J (1997) Extrusion tectonics and elevation of lower
1077 crustal metamorphic rocks on convergent orogens. Geology 25: 491–494.
1078 Tricart, P. 1984. From passive margin to continental collision - a tectonic scenario for the
1079 Western alps. American Journal of Science 284, 97-120.
1080 Tricart, P. and Sue, C., 2006. Faulted backfold versus reactivated backthrust: the role of
1081 inherited structures during late extension in the frontal Piedmont nappes east of Pelvoux
1082 (Western Alps). International Journal of Earth Sciences, 95, 827-840.
1083 Vidal O., Goffé B., Theye T. 1992. Experimental investigation of the stability of sudoite and
1084 magnesiocarpholite and calculation of a petrogenetic grid for the system FeO-MgO-
1085 Al2O3-SiO2-H2O. Journal of metamorphic geology, 10, .603-614.
1086 Vidal O., Goffé B, Parra T., Bousquet R. 1999. Calibration and testing of an empirical
1087 chloritoid-chloriteMg-Fe thermometer and thermodynamic data for daphnite. Journal of
1088 metamorphic geology, 17, 25-39.
1089 Vidal, O. and Parra, T. 2000. Exhumation paths of high pressure metapelites obtained from
1090 local equilibria for chlorite-phengite assemblages. Geological Journal, 35(3/4), 139-161.
1091 Vidal, O., Parra, T. and Trotet, F 2001. A thermodynamic model for Fe-Mg aluminous
1092 chlorite using data from phase equilibrium experiments and natural pelitic assemblages in
1093 the 100-600°C, 1-25 kbar P-T range. American Journal of Science. 301, 557-592.
1094 Vidal, O., Parra T., Vieillard. 2005. Experimental data on the Tscherrmak solid solution in
1095 Fe-chlorites: Application to natural examples and possible role of oxidation. Am.
1096 Mineral., 90, 359-370.

1097 Wheeler, J., Reddy, S. M. and Cliff, R. A., 2001. Kinematic linkage between internal zone
1098 extension and shortening in more external units in the NW Alps. Journal of the Geological
1099 Society of London.158, 439-443.
1100
1101

Figure Captions

Figure 1: Structural context of the studied area. **Inset map**: general context of the western Alpine belt. E.A. external Alps, E.F. European forland, I.A. internal Alps, M.S. Mediterranean sea. The frame locate the main map. **Main map**. Main units of the central Western Alps. Am.: Ambin, D.M.: Dora-Maira, G.P. Gran Paradiso, N.V.: Northern Vanoise, P.P.: Po plain, Sa: Sapey, S.V. : Southern Vanoise. The frame corresponds to the studied area (Figures 2 and 5) .

Figure 2: Structural scheme of the studied area, based on field data acquisition and previous maps (Debelmas et al., 1989, Ganne et al., 2005 and Gerber 2008). The different units are distinguished from lithologic, tectonic and metamorphic criteria (see text for more information).

Figure 3: Schematic stratigraphic section of the Modane-Aussois area.

Figure 4: Field observations. Structures related to the D1 and D2 events are labelled S0, S1 and S2 respectively. F1 and F2 correspond to the first (D1) and a second (D2) generation of folds. **A**: interbeded layering preserved in white quartzite. Such structures allow to determine the series polarity. **B**: carbonate lenses folded during D1 deformation phase in Permian conglomerate of the Modane-Aussois unit. **C**: C-S structure related to the D2 deformation phase in Ambin micaschists of the Modane-Aussois unit, a top to the east sense of shear is inferred. **D**: D2 folds with S2 axial foliation affecting the S1 schistosity. **E**: D1 folds and associated D1 vertical foliation preserved within the Clarea unit of the Southern Vanoise Unit. **F**: contact between the Clarea and Ambin groups of the Southern Vanoise unit affected by two generations of fold.

Figure 5: Geological map of the Modane-Aussois area. Black dot: location of the samples. White dots: position of the Lyon Turin Project drillholes

Figure 6: cross sections across the Modane-Aussois area. Drawn from field work and boreholes analysis. Surface samples and drillholes are located. See Fig. 5 for legend and location.

Figure 7: Photographs and structural interpretation of samples from Drillholes, illustrating the importance of D2 phase of deformation in the Briançonnais basement.. **A**: borehole F21-6, 780m depth. **B**: borehole F22-1, 567m depth. **C**: borehole F56-7, 623m depth. I: Inclination of the borehole.

Figure 8: Structures geometry. Stereographic projections, lower hemisphere. **A**) D1 stretching lineation on the Modane-Aussois unit. **B**) Same as A) but rotated to pre D2 geometry, taking into account local D2 deformations and late tilting (table 1). **C)**: Bedding poles from the Bourget du rock folds. From the 120 measurements a fold axis striking N18-21°S is calculated. **D**) D2 fold axes (square) and poles of D2 schistosity planes (dots) of the Modane-Aussois Unit. **E**) D1 schistosity planes (dots) in the Southern Vanoise Unit. From the 28 measurements a D2 fold axis striking N31-07°S is calculated. **F**) Poles of D2 foliation in the Southern Vanoise Unit (31 measurements).

Figure 9: Microphotographs of mineral paragenes observed in thin section. Left Natural light, rigth cross polarized light. **A)**: garnet, glaucophane and chlorite relationship within the Clarea basement of Southern Vanoise unit (sample M278). B and C: S1 and S2 foliations within the Clarea group of the Modane-Aussois unit (sample M266). D: S1 and S2 foliations within the Ambin group of the Modane-Aussois unit (sample F21-5).

Figure 10: A and B: BSE images of M278 sample (Clarea group, South Vanoise unit) thin section showing the relationship between late growth of chlorite (Chl) and Garnet (Gt), Glaucophane (Gl), Albite (Ab), phengite and Quartz (Qz). C: chemical map of the M278 sample showing the chemical heterogeneity of chlorite (Si content), Phengite (Si content) and garnet (Fe content).

Figure 11: Chemical map showing Al contents of the sample M290, (Ambin group, Modane-Aussois unit); Chlorite is displayed in red to orange, phengite in light blue to dark blue, albite in grey. Relics of the D1 foliation are preserved within albite phenocryst and in the matrix; it is associated with Si rich phengite. D1 foliation is folded with D2 foliation in the matrix axial plane. D2 foliation is underlined by low Si phengites, while some D1 phengites have been rotated parallel to D2..

Figure 12: **A**) composition of sample M278 garnets. Almandine, pyrope, grosular + spessatine ternary plot. Fields for alpine and pre-alpine garnet are after Ganne et al. (2003). **B,C,D** : Si vs Na diagrams of phengite for Modane-Aussois unit, and, Modane-Aussois unit (dated samples) and Southern Vanoise Unit basement. Phengites from basement rocks display a wide range of chemical composition depending on structural position of mineral whereas phengite of the Modane-Aussois unit cover have a more constant chemical composition.

Figure 13 : P-T projection for the system containing Na, Fe, Mg, K, Ca, Si Al based on the solution model of Powell and Holland (1998). **A** sample M266 (Modane-Aussois unit **B**) F21-5 (Modane-Aussois unit) and **C)** M278 (Southern Vanoise Unit). D1 stability fields are presented in dark and the D&-D2 transition is estimated. Dots and squares correspond to local chlorite-phengite equilibria along D2 foliation and around garnet respectivelly. Bulk chemical composition of sample is presented in table 3.

Figure 14: results of Ar^{39}/Ar^{40} dating of samples M80, M173 and M196 : microphotograph (A, B, C) and Ar^{38}/Ar^{39} (D, E, F), Ar^{37}/Ar^{39} (G, H, I), Ar^{39}/Ar^{40} age (K,L,M) spectra on phengites during step-wise heating. Arrows indicate the plateau ages.

Figure 15: **A**) Schematic cross section of the studied area showing the relationship between the Piemonte Unit (Pu), the Southern Vanoise Unit (Svu), the Dent Parrachée Unit (Dpu) and the Modane-Aussois unit (Mau). **B**) alpine Pressure Temperature Deformation path for the Piedmonte unit (after Agard et al., 2002), Southern Vanoise unit and Modane-Aussois unit (This study). **C)** Pressure Time Deformation paths for the Piedmont zone (Pu after Agard et al., 2002), Southern Vanoise unit (this study) and Modane-Aussois unit (this study). Time constrains of the Southern Vanoise unit are after Gerber (2008).

Figure 16 : Possible evolution along an E-W cross section of the western Alps between 50 and 30 Ma. Based on the P-T-t-d path for the Piedmonte zone (Agard et al., 2002), the Southern Vanoise Unit (this study, Ganne et al., 2007 and Gerber 2008) and the Modane-Aussois unit (this study). See text for discussion.

	Folded D1 Lineation			Unfolded D1 Lineation			D2 fold		late tilting	
point	Azimut	pendage	Dip Dir.	Azimut	pendage	Dip Dir.	Azimut	angle	Azimut	angle
1	74	15	E	92	18	E	30	8	90	30
2	110	2	E	130	14	E	30	20	90	20
3	114	22	E	114	22	E	30	0	90	0
4	56	80	E	115	10	E	30	80	90	0
5	146	48	E	138	22	E	30	35	90	0
6	154	48	E	100	24	E	30	60	90	30
7	124	14	E	124	14	E	30	0	90	0
8	158	24	E	158	24	E	30	0	90	0
9	18	16	W	138	4	E	30	90	90	30
10	50	38	W	142	20	E	30	85	90	20

Table 1 : folded and unfolded orientation of D1 mineral lineation. Dip Dir. : Dip Direction.

Mineral	Chl	Chl	Phe	Phe	Phe	Phe	Phe	Phe	Phe	Chl	Phe	Gt	Gl	Gl
TP	D1	D2	D1	D1	D2	D2	D2	D-1	D2	D2	D1	D1	D1	D1
Sample	F21-5	F21-5	F21-5	M80	M290	M173	M196	M290	M196	M278	M278	M278	M266	M278
SiO2	27.70	26.94	51.83	49.65	48.67	47.42	49.22	45.55	49.22	25.14	50.16	37.72	57.11	56.61
TiO2	0.09	0.04	0.31	0.20	0.10	0.66	0.52	0.17	0.52	0.06	0.17	0.08	0.00	0.12
Al2O3	23.81	23.74	30.09	29.80	29.05	26.04	27.22	27.73	27.22	20.39	26.64	20.85	10.66	11.89
FeO	25.26	26.06	2.40	1.72	5.11	6.72	4.90	5.98	4.90	31.80	3.50	31.61	17.65	16.48
MnO	0.08	0.00	0.00	0.02	0.00	0.01	0.01	0.00	0.01	0.42	0.01	0.32	0.07	0.07
MgO	10.95	11.11	2.38	2.27	2.44	1.71	2.14	3.90	2.14	10.29	2.98	1.24	5.46	5.30
CaO	0.01	0.00	0.00	0.03	0.04	0.02	0.00	0.01	0.00	0.04	0.00	8.60	0.04	0.18
Na2O	0.04	0.11	0.49	0.09	0.17	0.05	0.10	0.16	0.10	0.09	0.20	0.04	6.76	7.19
K2O	0.93	0.91	10.75	11.14	10.64	11.34	11.25	9.95	11.25	0.05	10.66	0.00	0.00	0.03
Total	88.88	88.91	98.25	94.93	96.22	93.97	95.37	93.46	95.37	88.28	94.31	100.47		
Si	2.79	2.74	3.34	3.32	3.24	3.28	3.32	3.16	3.32	2.64	3.40	3.01	8.08	7.97
Ti	0.01	0.00	0.01	0.01	0.01	0.03	0.03	0.01	0.03	0.00	0.01	0.00	0.00	0.01
Al	2.83	2.85	2.28	2.35	2.28	2.12	2.16	2.27	2.16	2.57	2.13	1.96	1.78	1.97
Fe	2.13	2.22	0.13	0.10	0.28	0.39	0.28	0.35	0.28	3.22	0.20	2.11	2.09	1.94
Mn	0.01	0.00	0.00	0.00	0.00	0.00	0.00	0.00	0.00	0.03	0.00	0.02	0.01	0.01
Mg	1.65	1.68	0.23	0.23	0.24	0.18	0.21	0.40	0.21	1.60	0.30	0.15	1.15	1.11
Ca	0.00	0.00	0.00	0.00	0.00	0.00	0.00	0.00	0.00	0.01	0.00	0.74	1.85	1.96
Na	0.01	0.02	0.06	0.01	0.02	0.01	0.01	0.02	0.01	0.02	0.03	0.01	1.85	1.96
K	0.12	0.12	0.88	0.95	0.90	1.00	0.97	0.88	0.97	0.01	0.92	0.00	0.00	0.00
ON	14	14	11	11	11	11	11	11	11	14	11	12	23	23

Table 2 : chemical composition of the main metamorphic mineral

	Southern Vanoise unit Clarea Group	Modane-Aussois unit Clarea Group
	Ma278	Ma266
SiO2	63.52	65.26
Al2O3	17.17	16.35
Fe2O3	6.74	5.57
MnO	0.07	0.05

MgO	2.02	1.85
CaO	0.24	0.55
Na2O	3.22	3.8
K2O	3.03	2.73
TiO2	0.78	0.71
P2O5	0.15	0.13
L.O.I.	2.82	2.78
H2O-	0.08	0.06
Total	**99.84**	**99.84**

Table 3 : bulk composition of samples used for pseudosection calculation.

	Piemonte Unit		**Southern Vanoise Unit**		**Modane Aussois Unit**	
Time	vertical motion	Tectonics	vertical motion	Tectonics	vertical motion	Tectonics
60-50 Ma	Burial	W thrusting	-	-	-	-
50-45 Ma	Exhumation	W thrusting	Burial	W thrusting	-	-
45-37 Ma	Exhumation	E Detachment	Exhumation	W thrusting	Burial	W thrusting
38-37 Ma	Exhumation	W Detachment	Exhumation	E	Exhumation	W thrusting
35-30 Ma	-	-	Exhumation	E	Exhumation	E

Table 4: Relationship throught tim between vertical motion and tectonic phase for the Piemonte, the Southern Vanoise and the Modane Aussois Units

Figure 1

Click here to download high resolution image

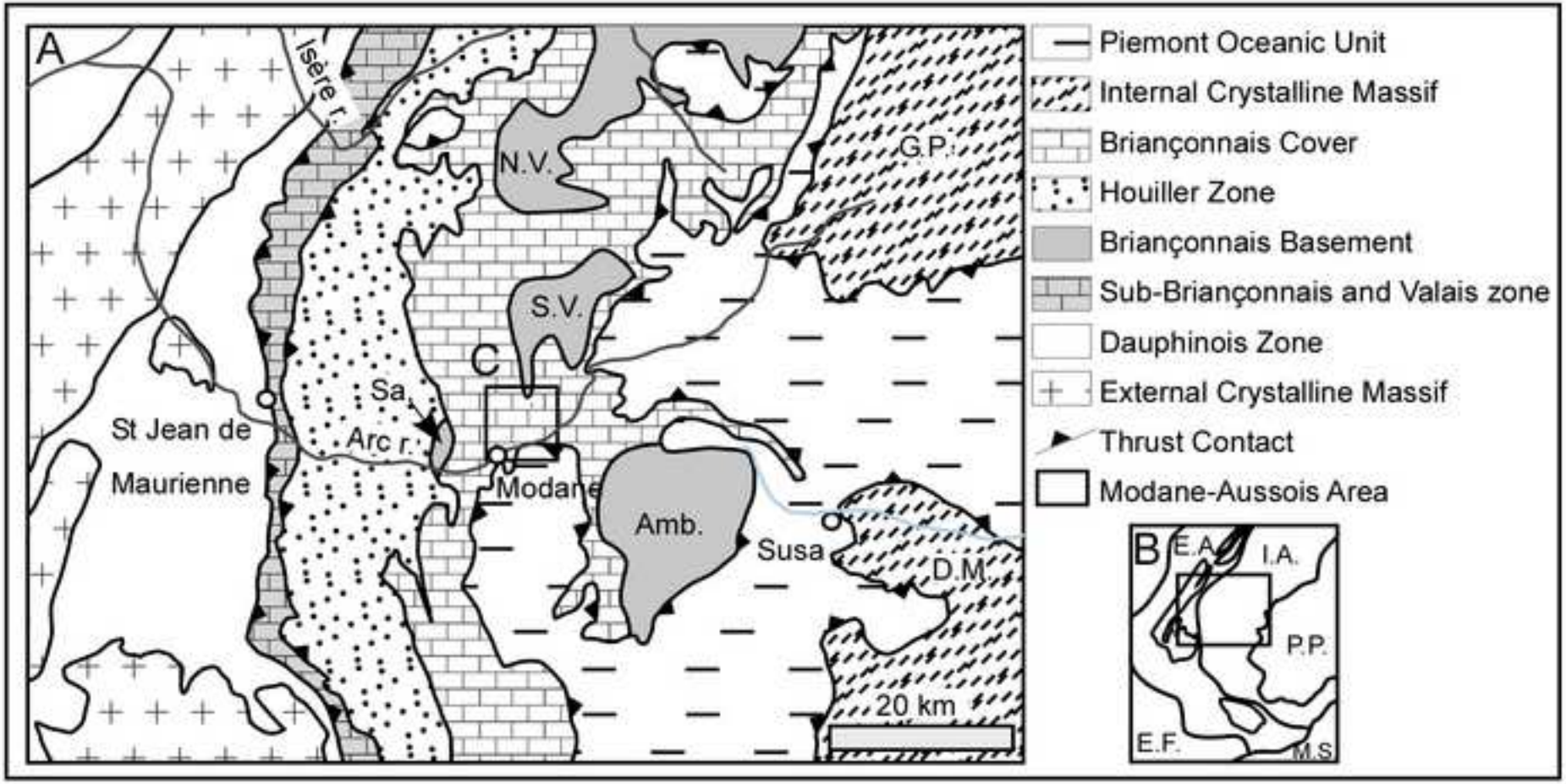

Figure 2

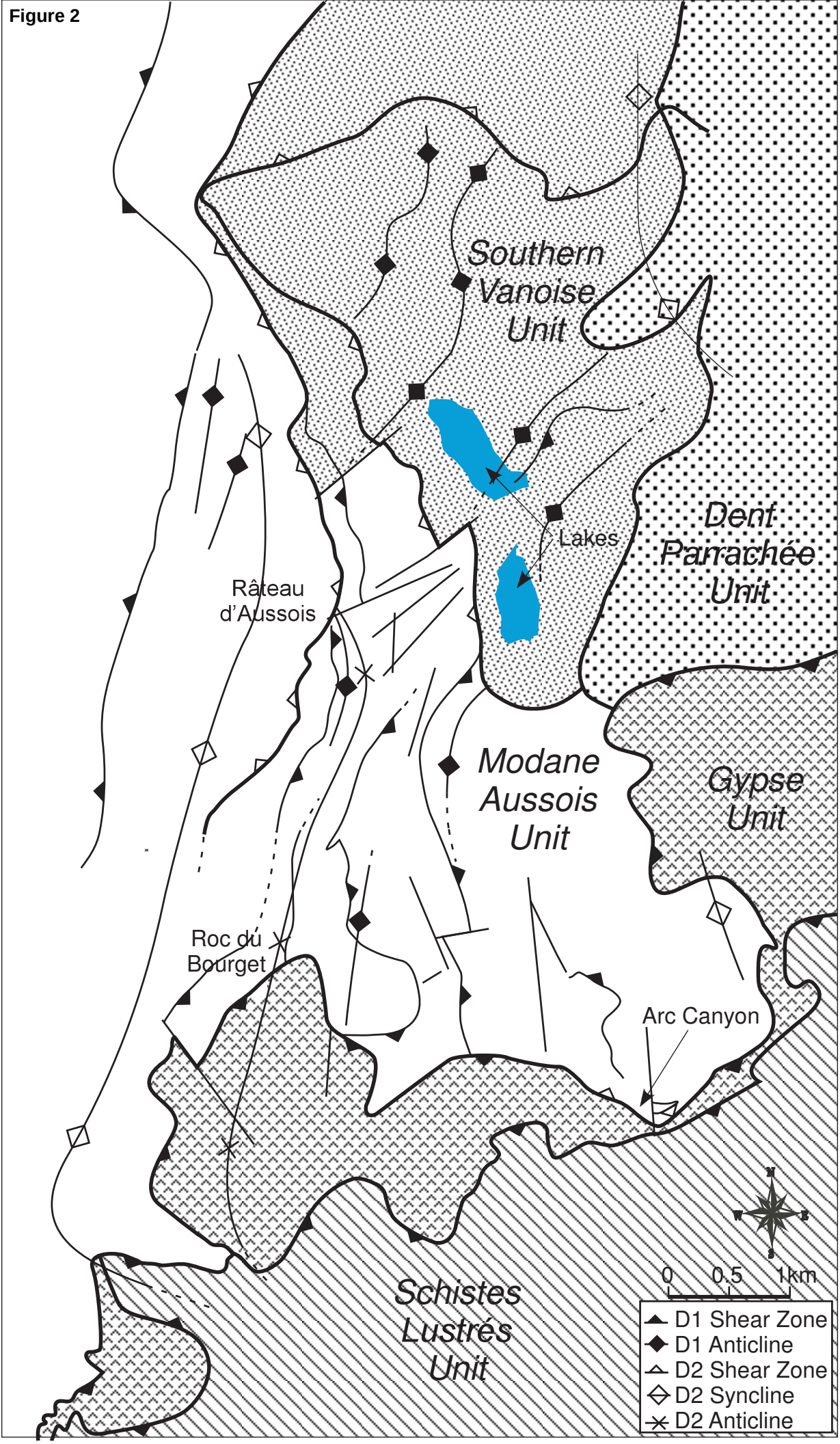
Southern Vanoise Unit
Dent Parrachée Unit
Lakes
Râteau d'Aussois
Modane Aussois Unit
Gypse Unit
Roc du Bourget
Arc Canyon
Schistes Lustrés Unit
N
W
E
S
0
0.5
1km
D1 Shear Zone
D1 Anticline
D2 Shear Zone
D2 Syncline
D2 Anticline

Figure 3

Click here to download high resolution image

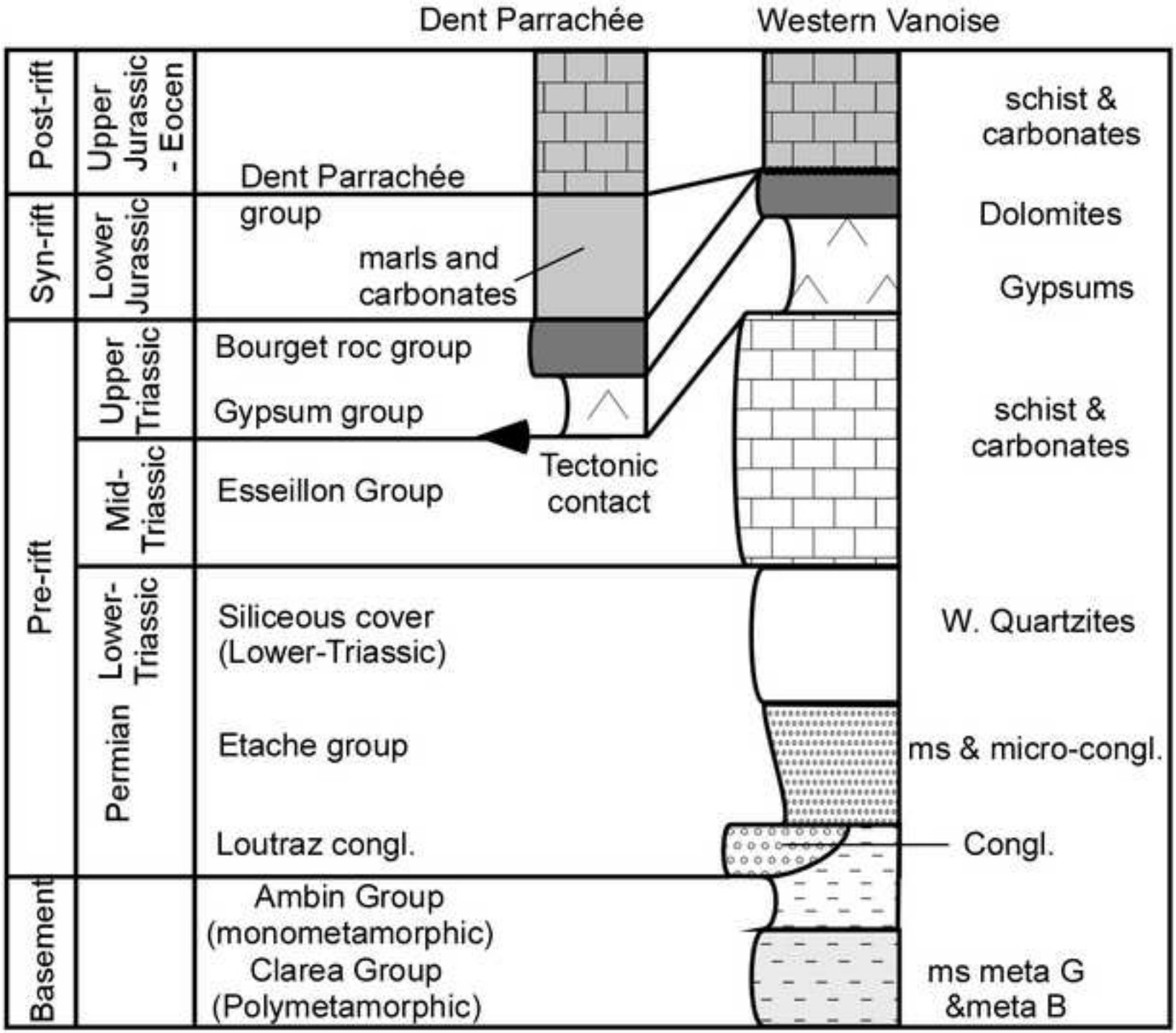

Figure 4

Click here to download high resolution image

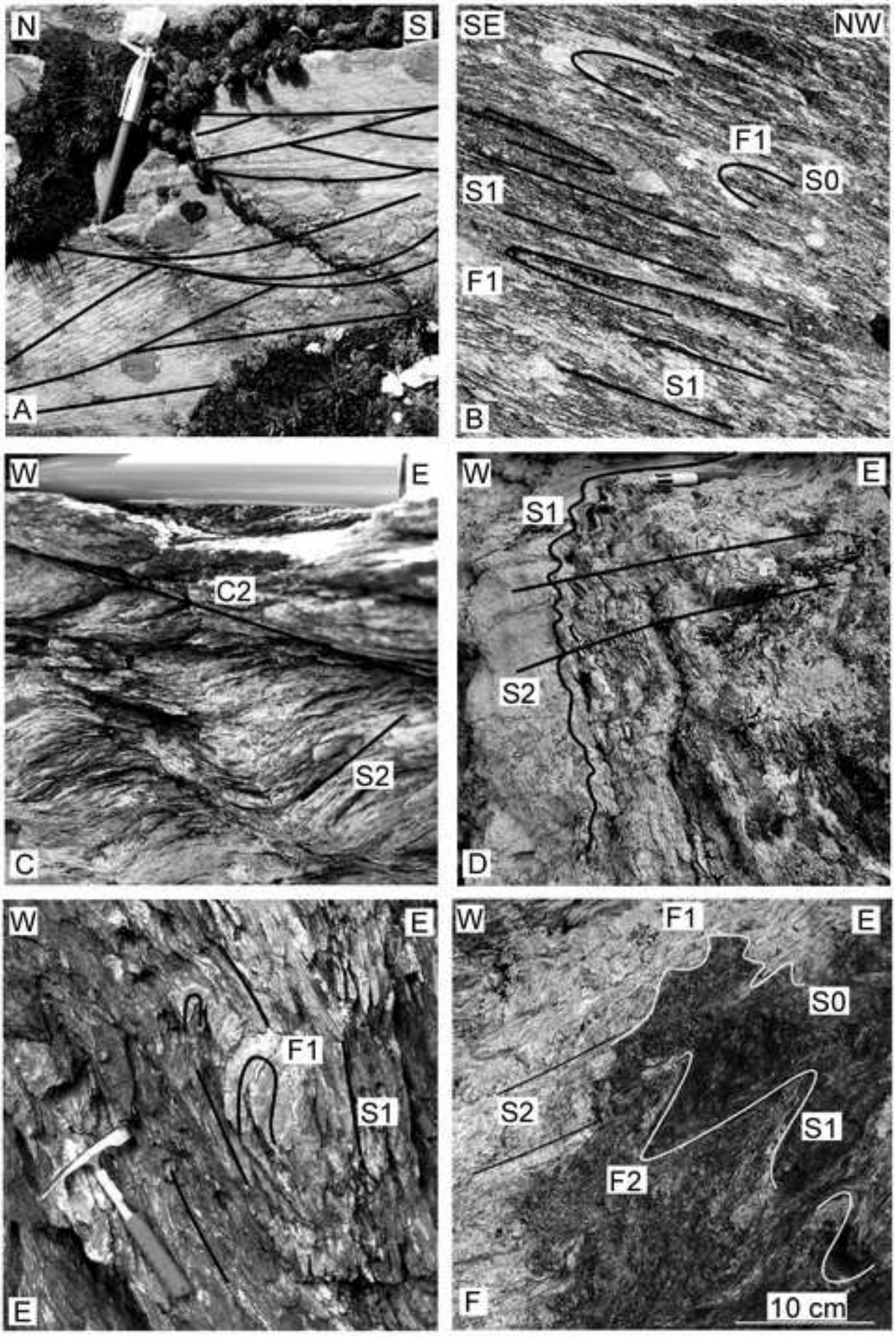

Figure 5

Click here to download high resolution image

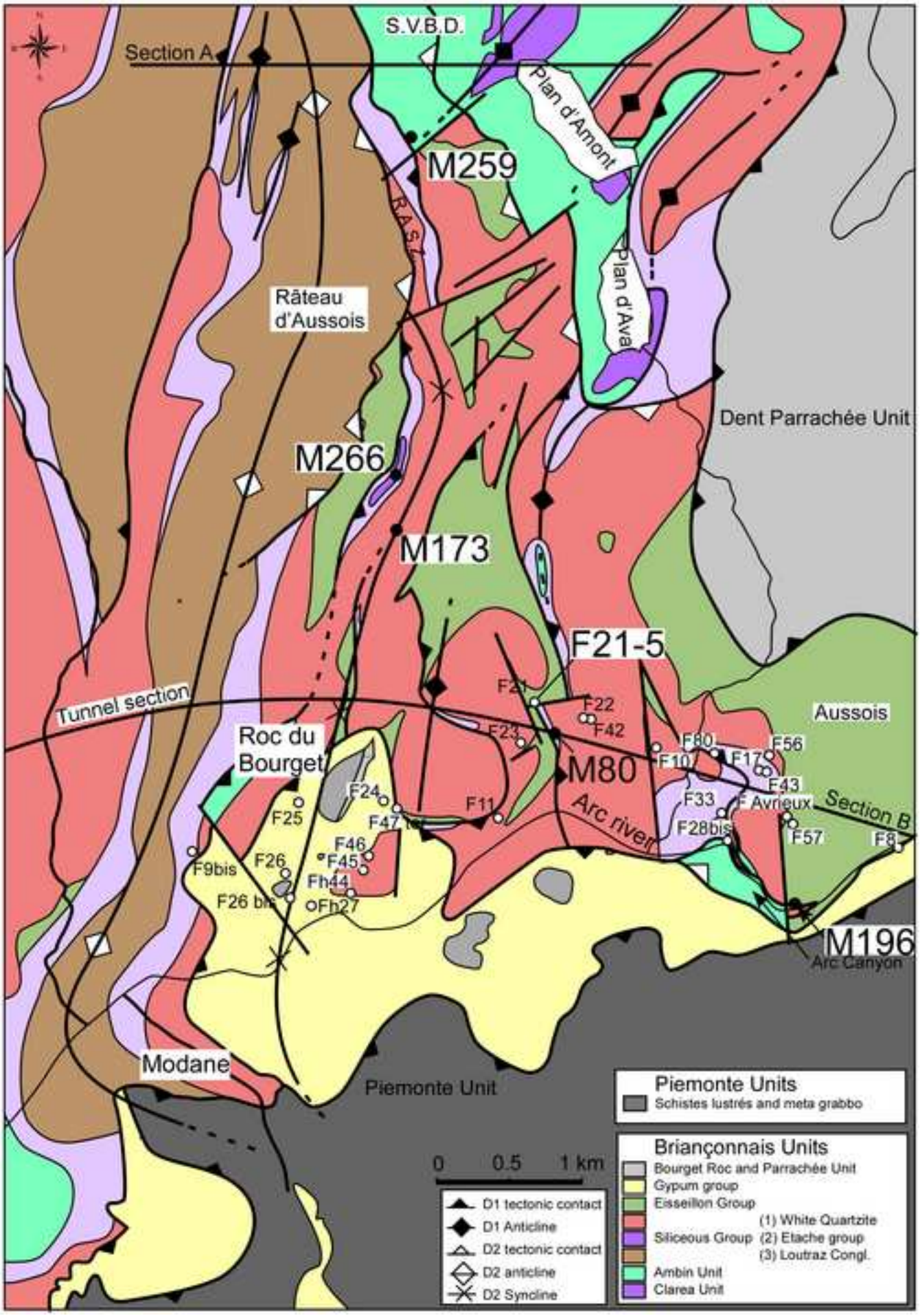

Figure 6

Click here to download high resolution image

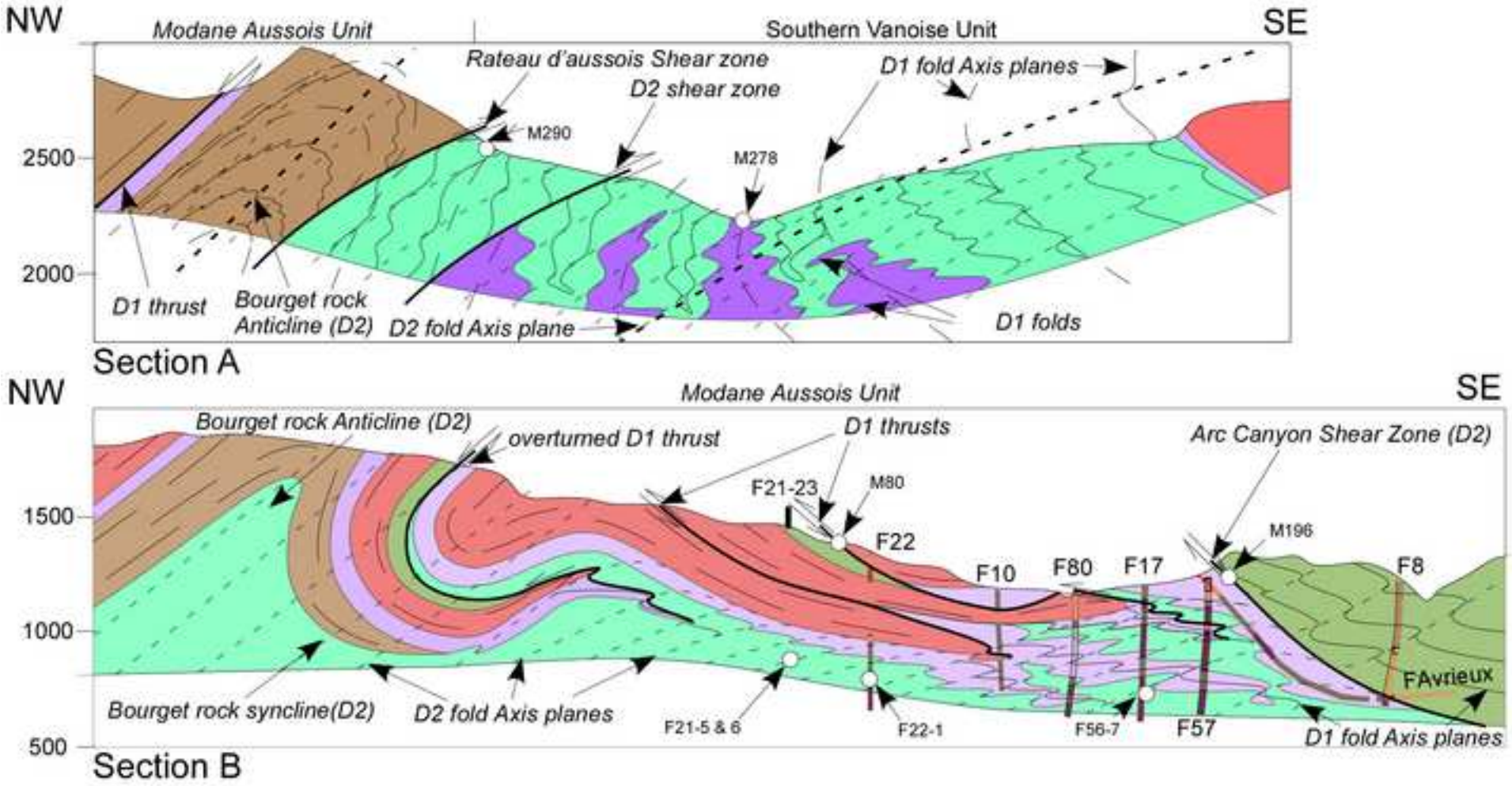

Figure 7

Click here to download high resolution image

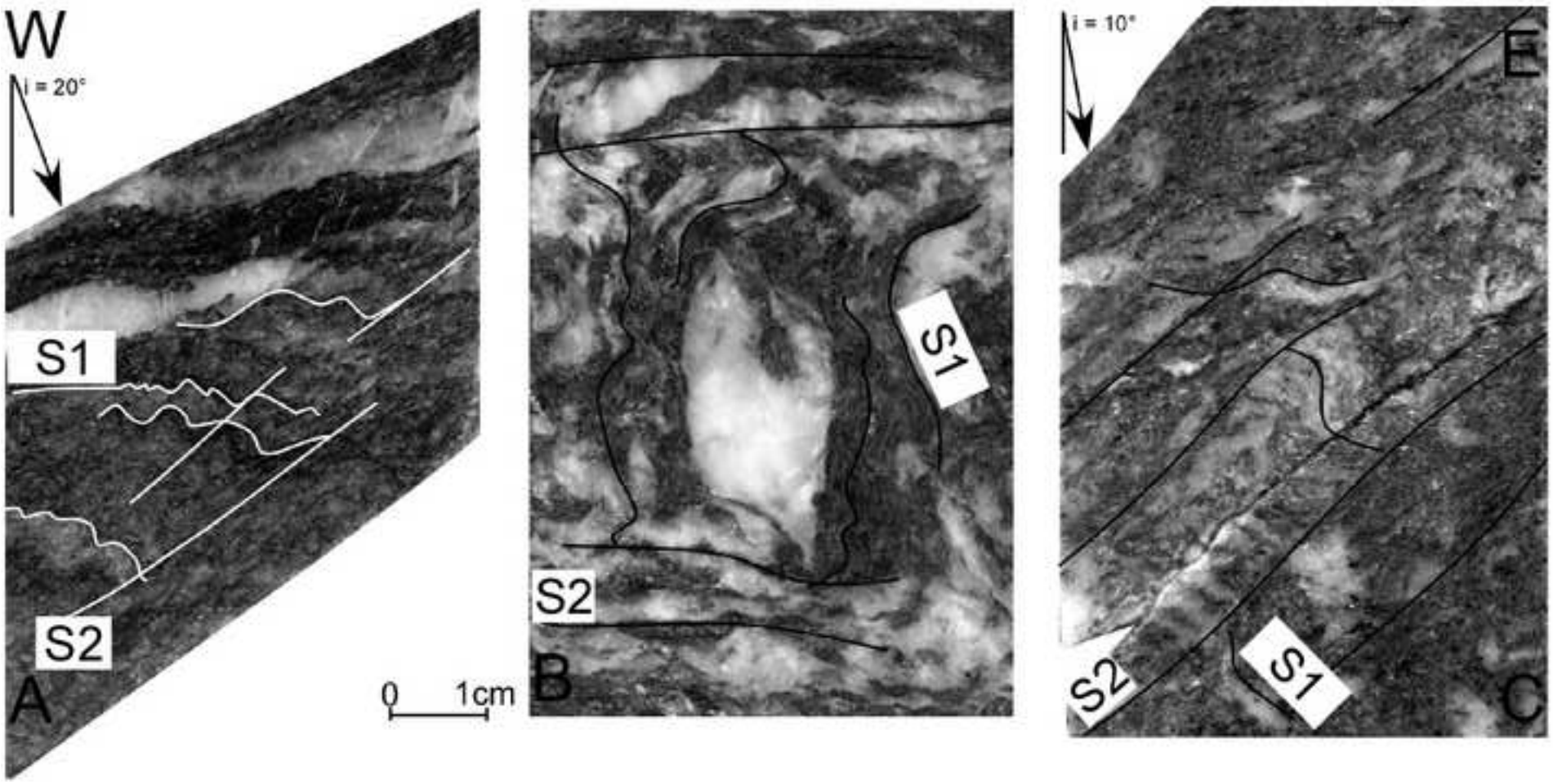

Figure 8

Click here to download high resolution image

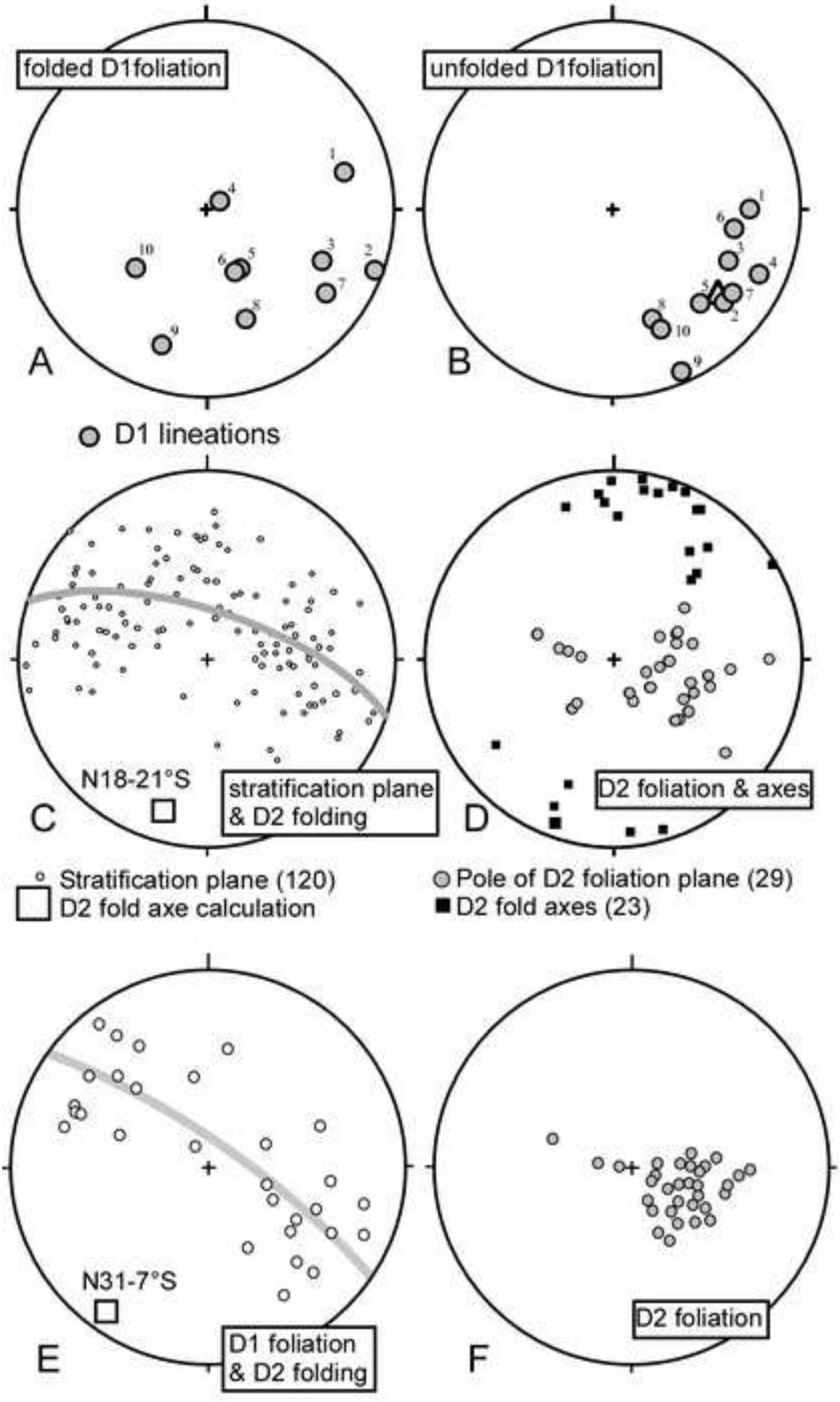

Figure 9

Click here to download high resolution image

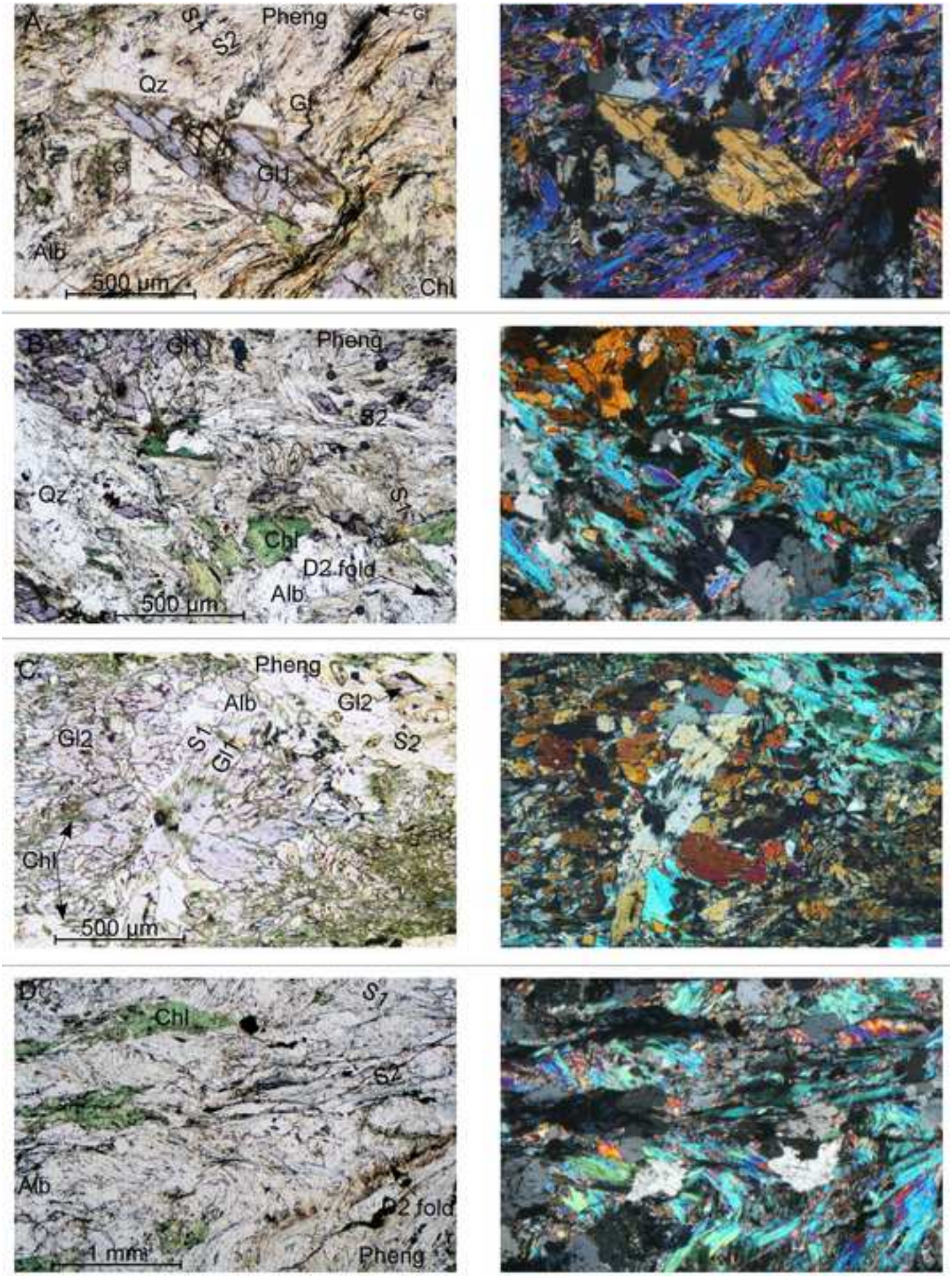

Figure 10

Click here to download high resolution image

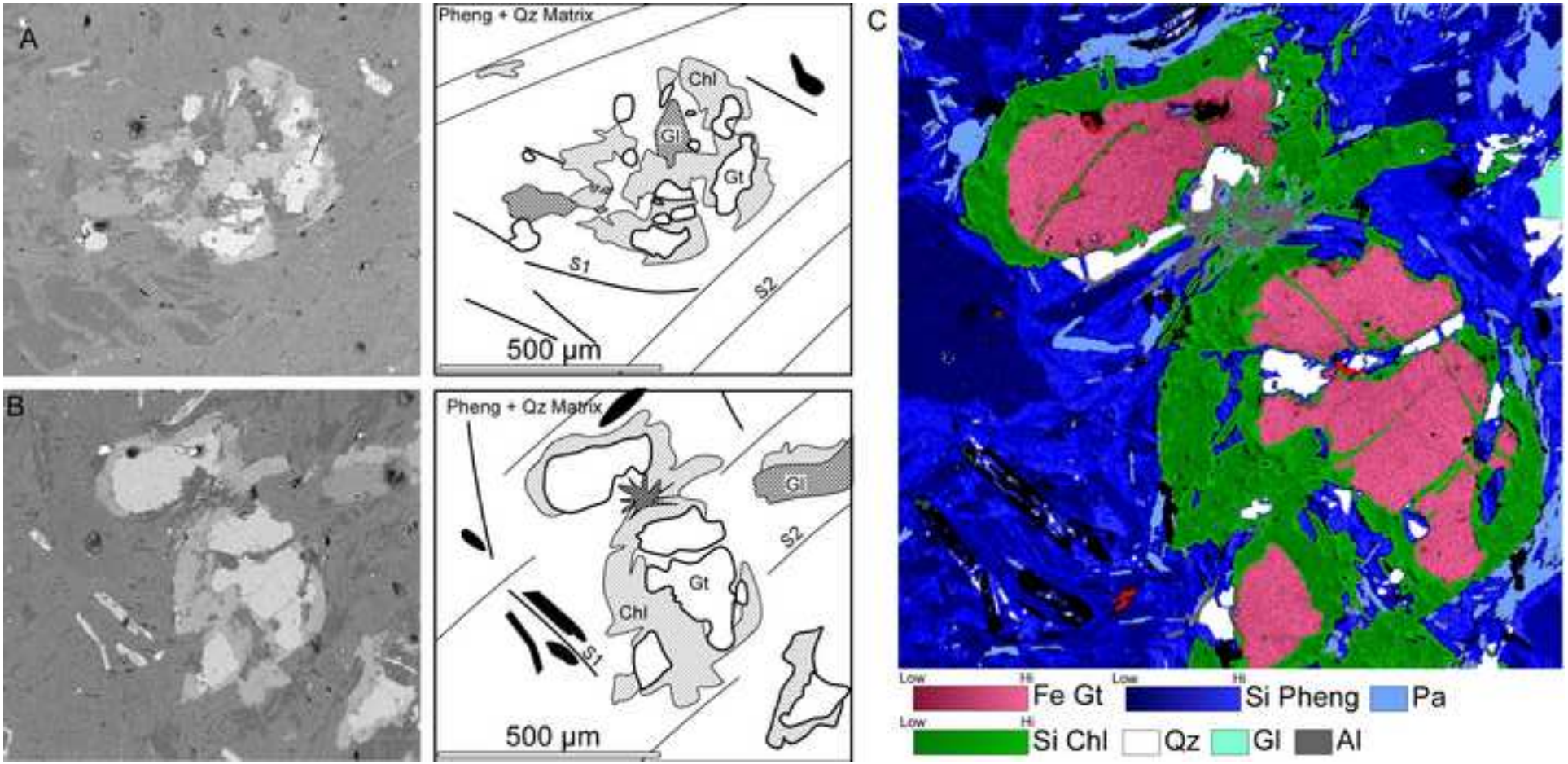

Figure 11

Click here to download high resolution image

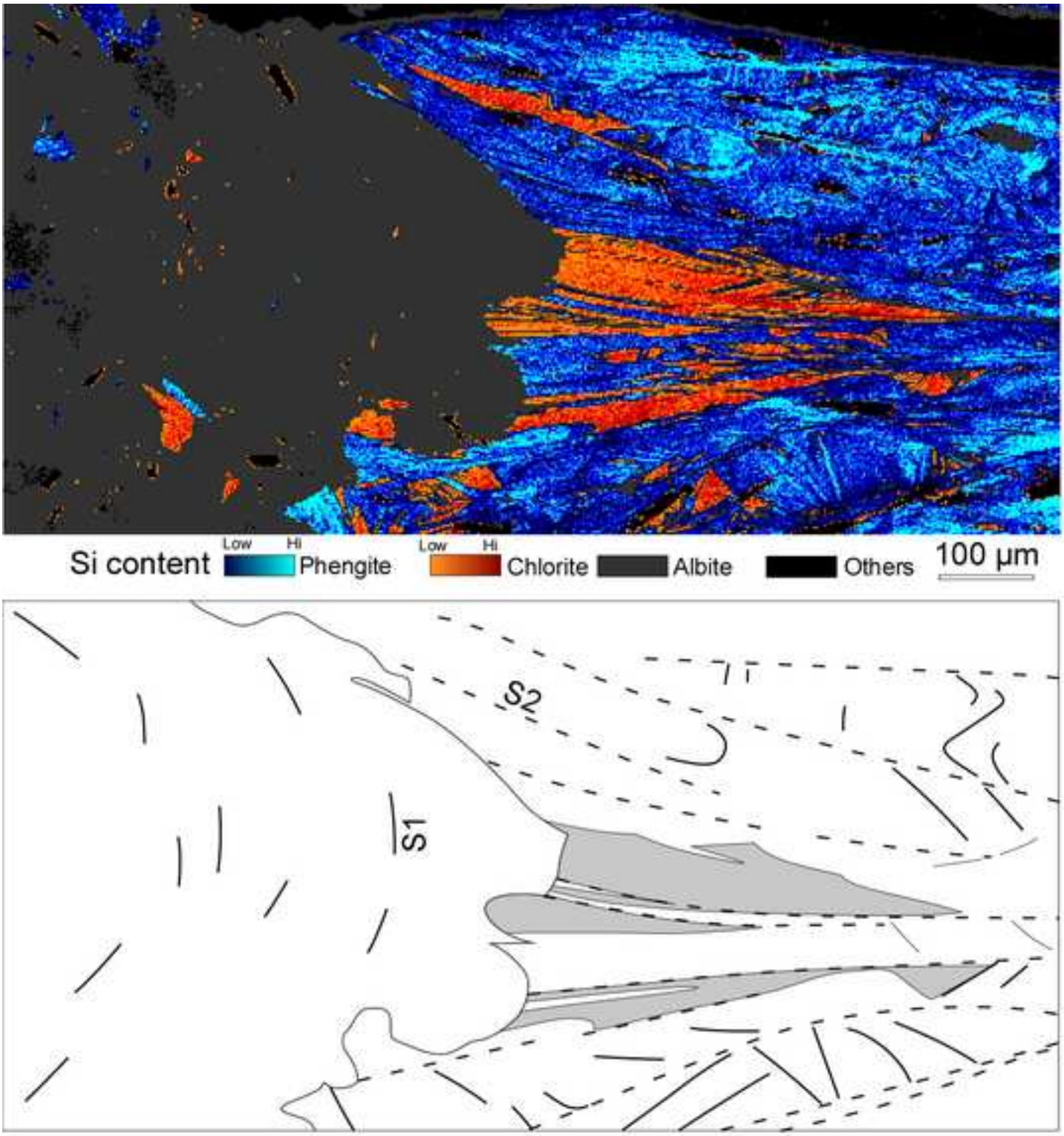

Figure 12

Click here to download high resolution image

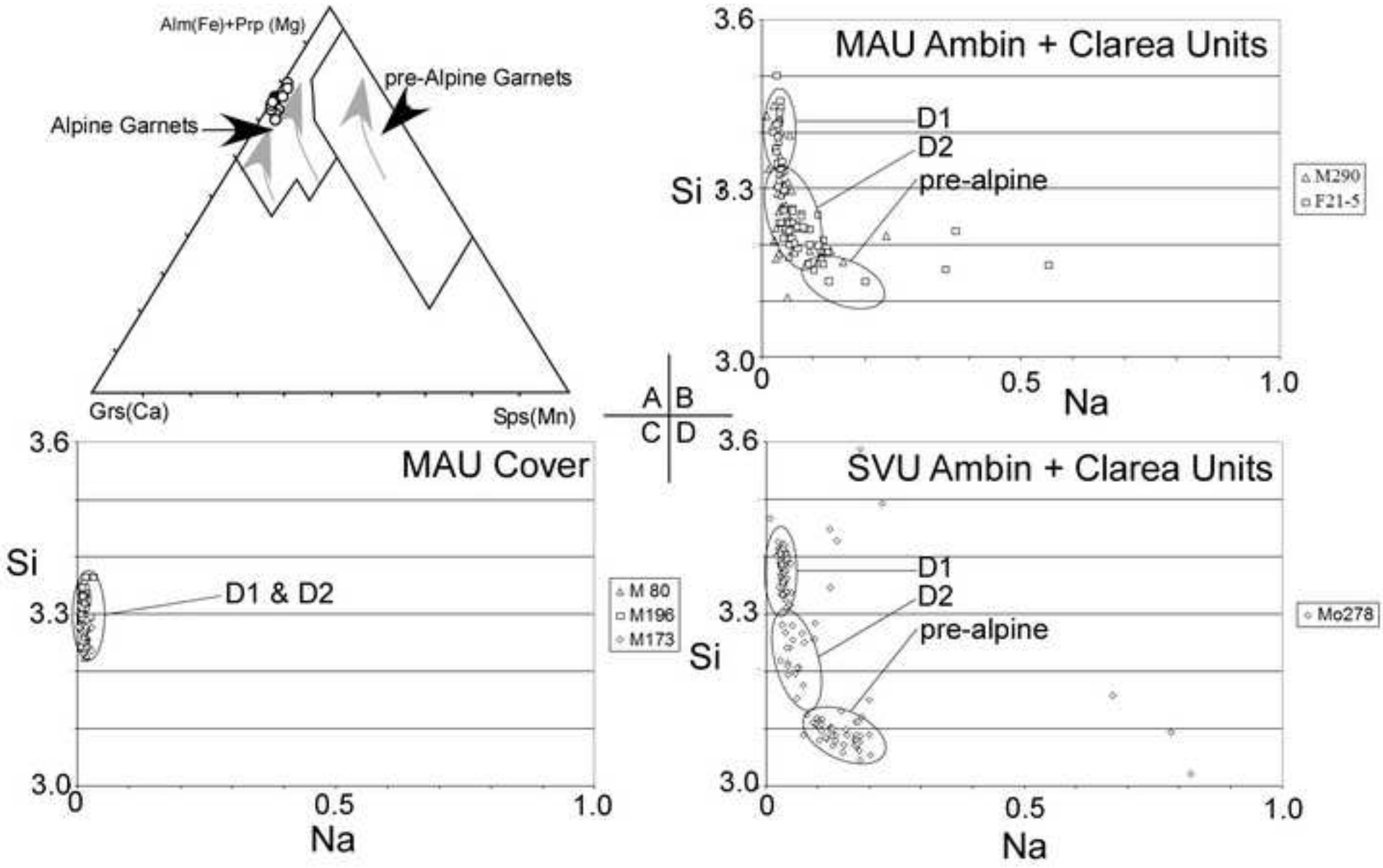

Figure 13

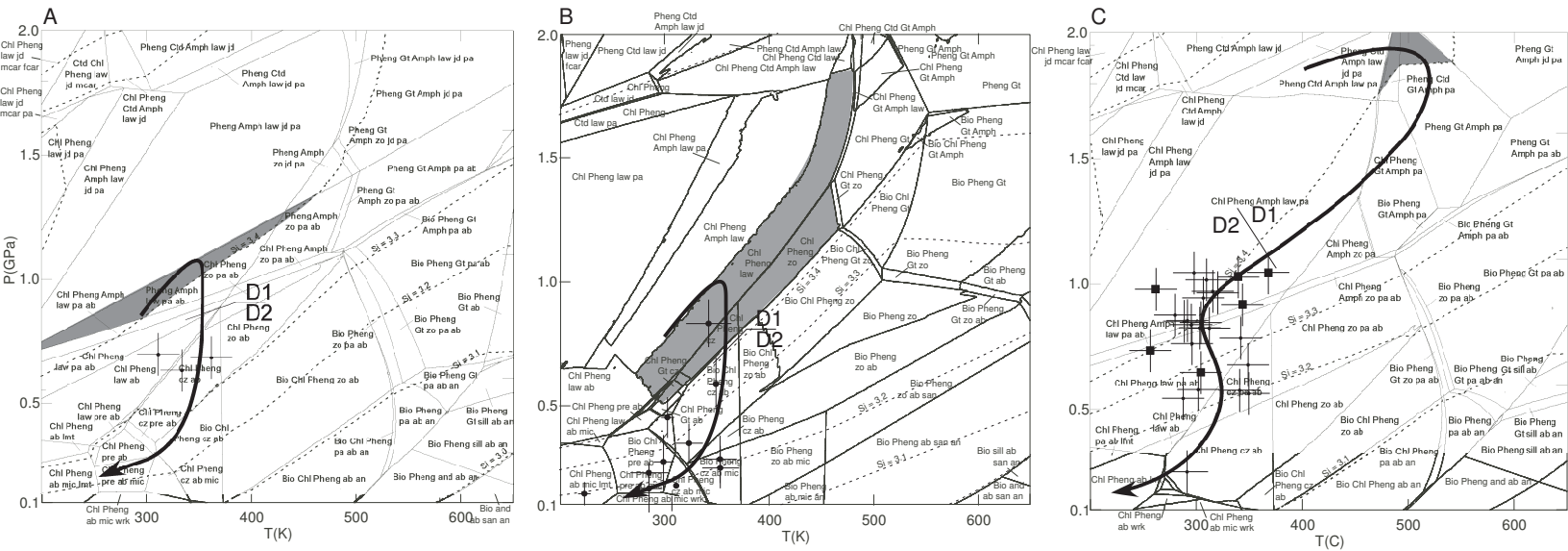

Figure 14

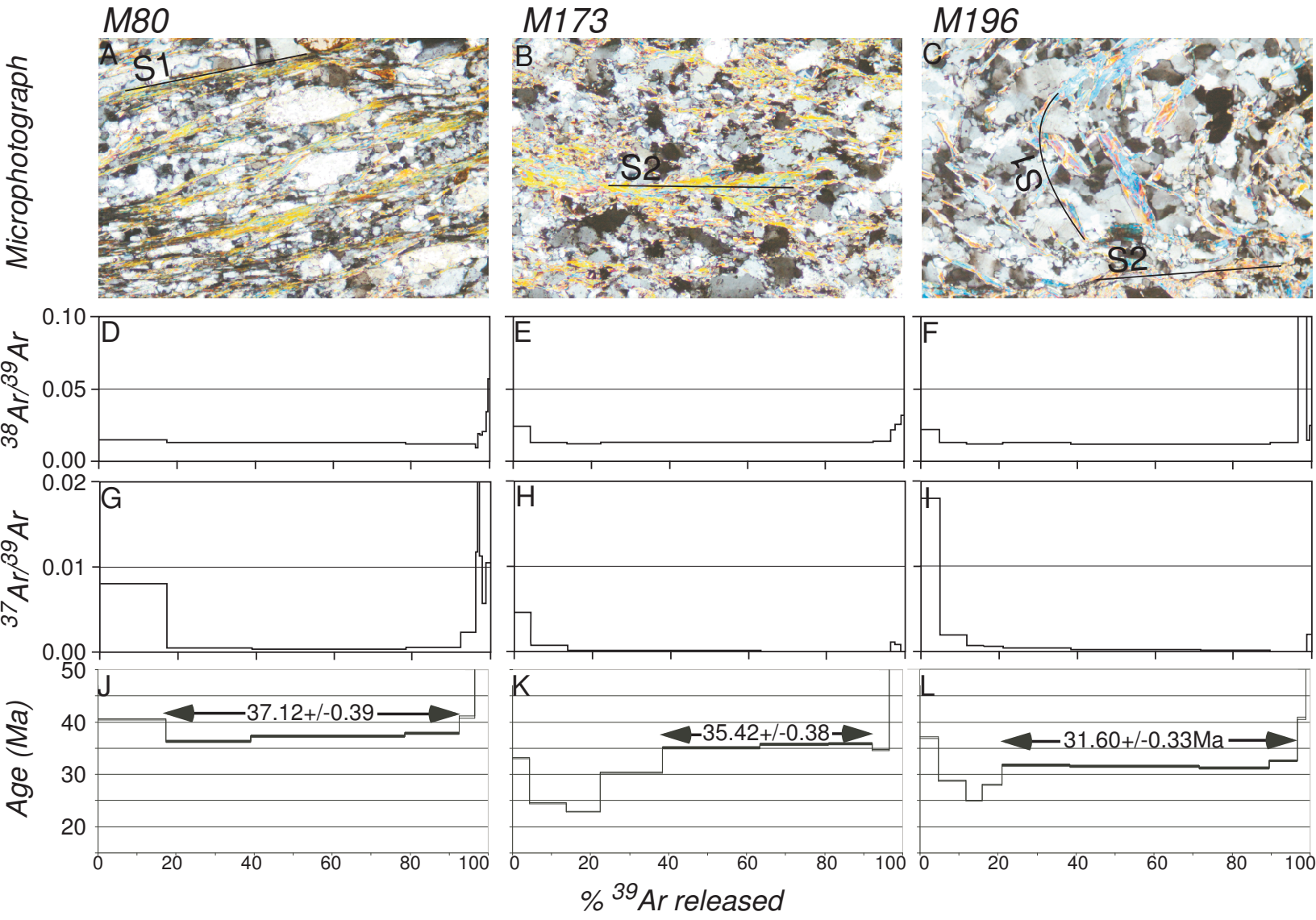
M80
M173
M196
Microphotograph
A
S1
B
S2
C
S1
S2
D
E
F
$^{38}Ar/^{39}Ar$
0.10
0.05
0.00
G
H
I
$^{37}Ar/^{39}Ar$
0.02
0.01
0.00
J
K
L
Age (Ma)
50
40
30
20
37.12+/-0.39
35.42+/-0.38
31.60+/-0.33Ma
0
20
40
60
80
100
% ^{39}Ar released

Figure 15

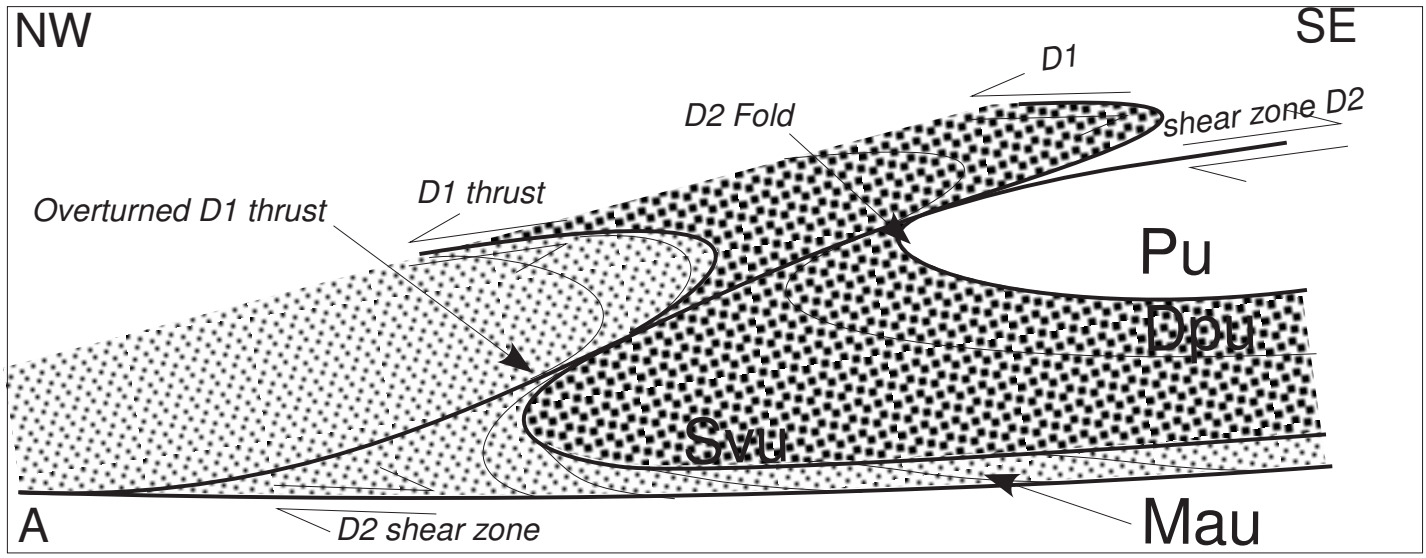
NW
SE
D1
D2 Fold
shear zone D2
Overturned D1 thrust
D1 thrust
Pu
Dpu
Svu
Mau
A
D2 shear zone

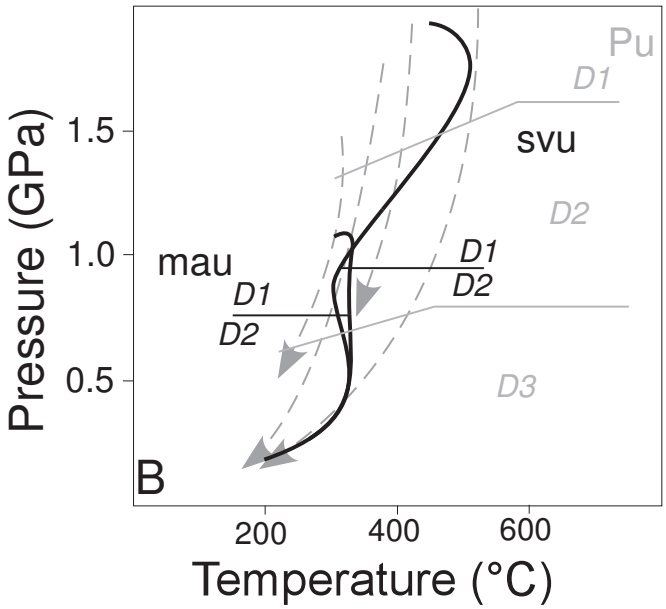
Pu
D1
svu
D2
mau
D1
D2
D1
D2
D3
B
Pressure (GPa)
1.5
1.0
0.5
200
400
600
Temperature (°C)

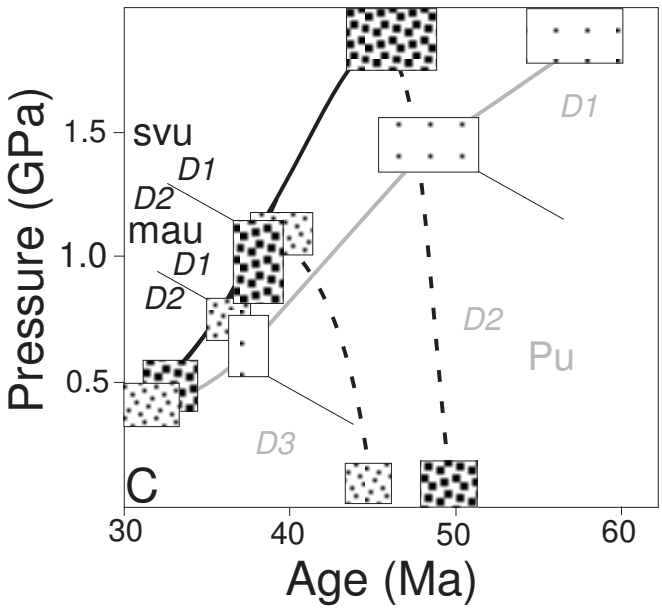
svu
D1
D2
mau
D1
D2
D1
D2
Pu
D3
C
Pressure (GPa)
1.5
1.0
0.5
30
40
50
60
Age (Ma)

Figure 16

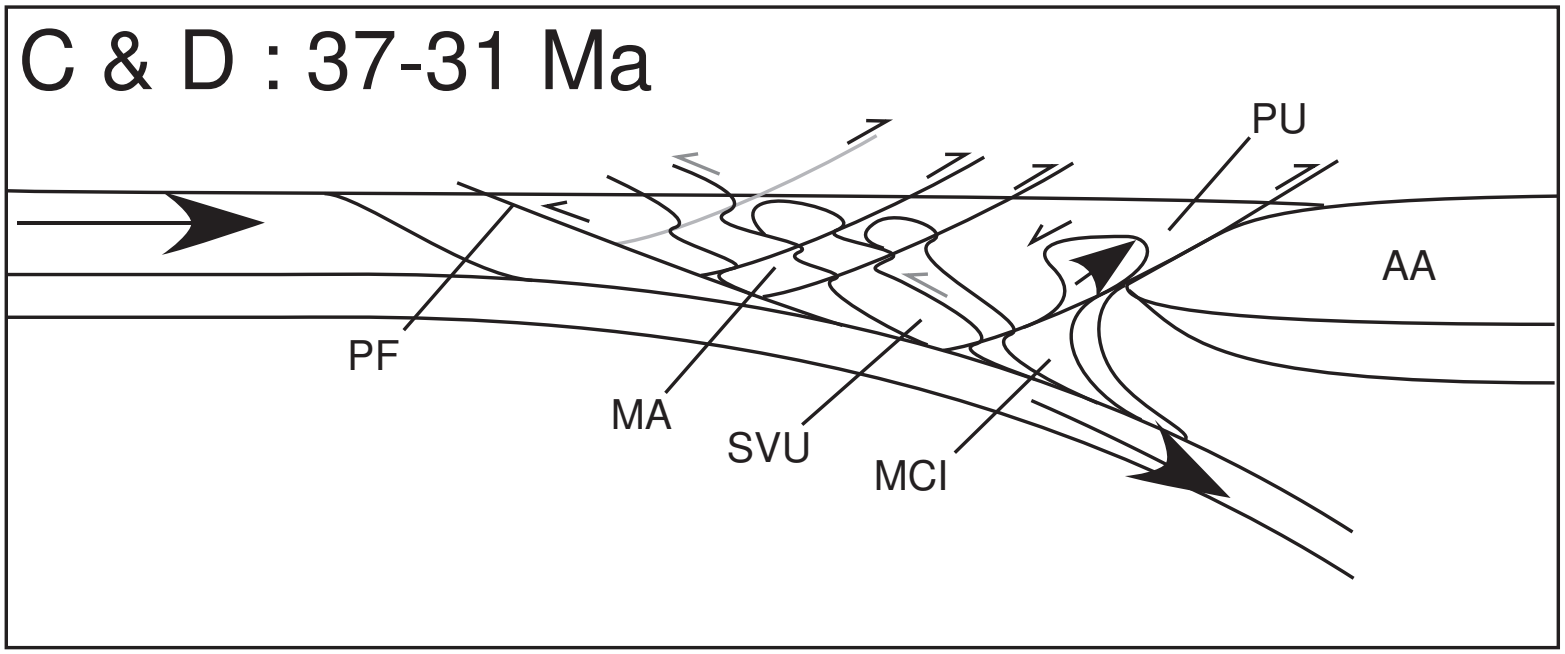
C & D : 37-31 Ma
PU
AA
PF
MA
SVU
MCI

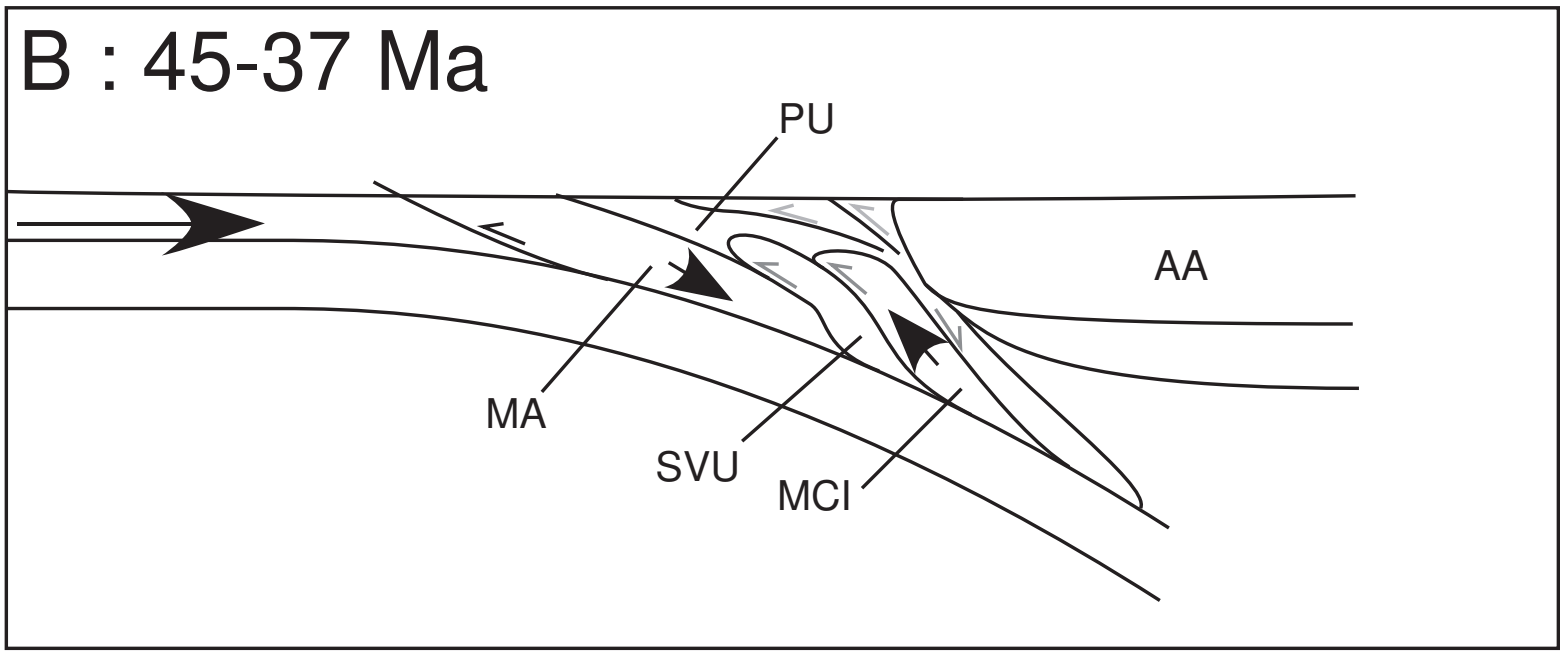
B : 45-37 Ma
PU
AA
MA
SVU
MCI

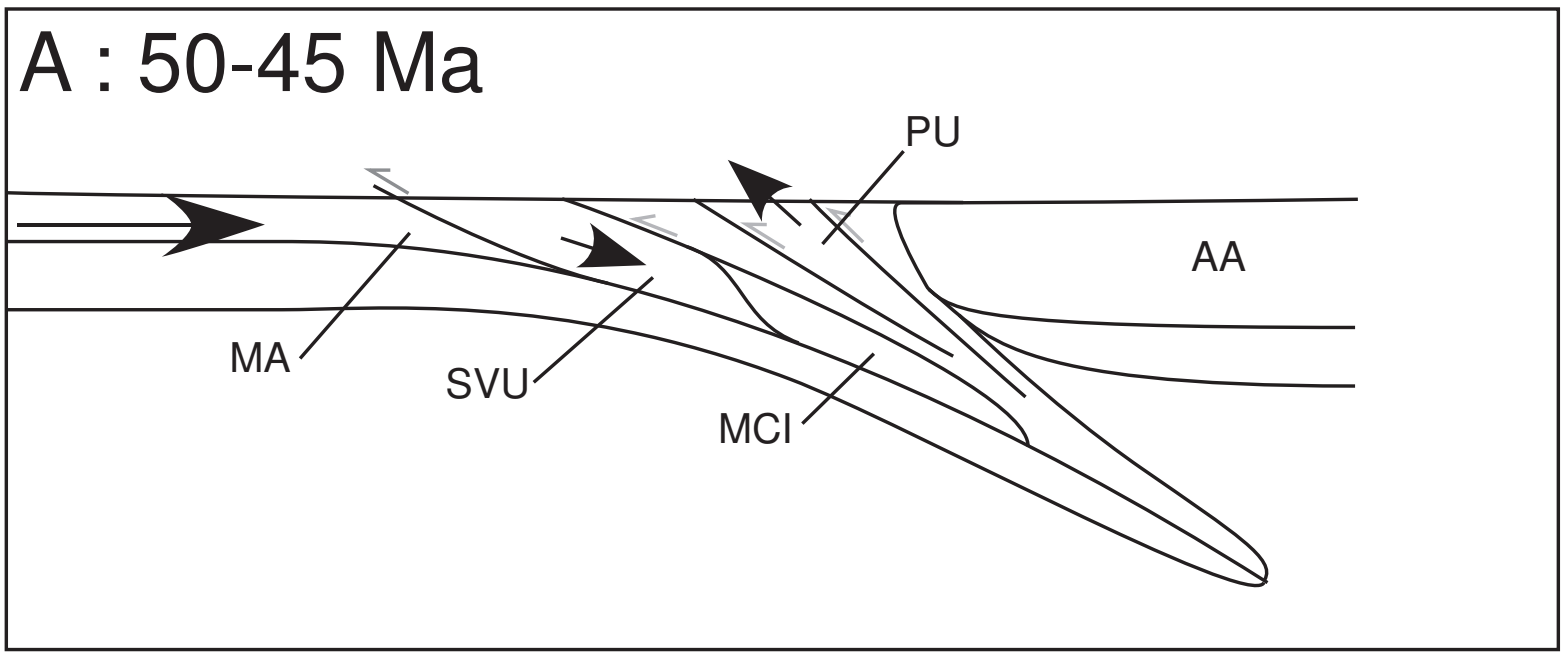
A : 50-45 Ma
PU
AA
MA
SVU
MCI